



HAL
open science

Modified reptile search algorithm for optimal integration of renewable energy sources in distribution networks

Ahmed Hachemi, Fares Sadaoui, Salem Arif, Abdelhakim Saim, Mohamed Ebeed, Salah Kamel, Francisco Jurado, Emad Mohamed

► To cite this version:

Ahmed Hachemi, Fares Sadaoui, Salem Arif, Abdelhakim Saim, Mohamed Ebeed, et al.. Modified reptile search algorithm for optimal integration of renewable energy sources in distribution networks. Energy Science & Engineering, 2023, 11 (12), pp.4635-4665. 10.1002/ese3.1605 . hal-04538467

HAL Id: hal-04538467

<https://hal.science/hal-04538467v1>

Submitted on 27 May 2024

HAL is a multi-disciplinary open access archive for the deposit and dissemination of scientific research documents, whether they are published or not. The documents may come from teaching and research institutions in France or abroad, or from public or private research centers.




L'archive ouverte pluridisciplinaire **HAL**, est destinée au dépôt et à la diffusion de documents scientifiques de niveau recherche, publiés ou non, émanant des établissements d'enseignement et de recherche français ou étrangers, des laboratoires publics ou privés.



Distributed under a Creative Commons Attribution 4.0 International License

ORIGINAL ARTICLE

Modified reptile search algorithm for optimal integration of renewable energy sources in distribution networks

Ahmed T. Hachemi¹  | Fares Sadaoui¹ | Salem Arif² | Abdelhakim Saim³ | Mohamed Ebeed⁴ | Salah Kamel⁵  | Francisco Jurado⁶  | Emad A. Mohamed⁷

¹Electrical Engineering Laboratory, University of Kasdi Merbah Ouargla, Ouargla, Algeria

²LACoSERE Laboratory, University of Amar Telidji, Laghouat, Algeria

³IREENA Laboratory, Nantes University, Saint Nazaire, France

⁴Department of Electrical Engineering, Faculty of Engineering, Sohag University, Sohag, Egypt

⁵Electrical Engineering Department, Faculty of Engineering, Aswan University, Aswan, Egypt

⁶Department of Electrical Engineering, University of Jaén, Jaén, Spain

⁷Department of Electrical Engineering, Prince Sattam Bin Abdulaziz University, Al Kharj, Saudi Arabia

Correspondence

Abdelhakim Saim, IREENA Laboratory, Nantes University, Saint Nazaire, France.
Email: Abdelhakim.Saim@univ-nantes.fr

Funding information

Université de Nantes,
Grant/Award Number: FR01

Abstract

This paper introduces a Modified Reptile Search Algorithm (MRSA) designed to optimize the operation of distribution networks (DNs) considering the growing integration of renewable energy sources (RESs). The integration of RESs-based Distributed Generation (DG) systems, such as wind turbines (WTs) and photovoltaics (PVs), presents a complex challenge due to its significant impact on DN operations and planning, particularly considering uncertainties related to solar irradiance, temperature, wind speed, consumption, and energy prices. The primary objective is cost reduction, encompassing electricity acquisition, PV and WTs unit costs, and annual energy losses. The proposed MRSA incorporates two strategies: the fitness-distance balance method and Levy flight motion, enhancing its searching capabilities beyond standard Reptile Search Algorithm and mitigating local optima issues. The uncertainties in load demand, energy prices, and renewable energy generation are represented through probability density functions and simulated using Monte Carlo methods. Evaluation involves typical benchmark functions and a real 112-bus Algerian DN, comparing MRSA's efficacy with other optimization techniques. Results indicate that the proposed DN optimization program with WTs and PVs integration reduces annual costs by 21.43%, from $6.2715E + 06$ to $4.9270E + 06$ USD, reduce voltage deviations by 21.67%, from 77.1022 to 60.4007 USD, and enhance system stability by 2.59%, from $2.3699E + 03$ to $2.4314E + 03$ USD, compared with the base case.

KEYWORDS

optimal distribution networks planning, optimal operation, renewable energy sources, reptile search algorithm, uncertainty

1 | INTRODUCTION

Renewable energy integration has become an increasingly important topic in recent years, as it offers many advantages in terms of reducing the environmental

impact of electricity generation. One of the most promising approaches is the optimal integration of renewable energy resources (RERs)-based Distributed Generations (DGs), such as wind turbine (WT), and photovoltaic (PV), into the distribution network (DN).

This is an open access article under the terms of the Creative Commons Attribution License, which permits use, distribution and reproduction in any medium, provided the original work is properly cited.

© 2023 The Authors. *Energy Science & Engineering* published by Society of Chemical Industry and John Wiley & Sons Ltd.

This approach presents multiple advantages, such as reducing greenhouse gas emissions, minimizing energy losses, improving voltage stability, and reducing the dependence on fossil fuels.

In this context, the optimization of RERs integration in DNs has gained significant attention in the literature, as it represents a crucial step towards achieving a sustainable and dependable energy system. For this aim, the integration of RERs-based DG units at different levels of the electrical networks has been recognized as a promising solution to address both the increasing demand for energy as well as to reduce the environmental impact. Additionally, the integration of such systems has shown multiple technoeconomic advantages reducing the total production cost of electricity, as well as enhancing system performance and voltage profiles.¹ However, the presence of DGs in DNs also introduces significant uncertainty, which greatly increases the intricacy of the optimal operation.² The main sources of uncertainty in DNs are the load demand, the prices of electricity, and the output power of renewable DGs, which are subject to variations depending on weather conditions (solar radiation, temperature, and wind speed). As a result, determining the optimal placement of DGs in DNs is a challenging and strenuous task.³ The selection of appropriate combinations of PV and WT-based DGs has the potential to increase the efficiency and reliability of the DNs by addressing the issues caused by their variable nature.⁴ DGs can be strategically located and operated in the network to defer major system upgrades, improve voltage regulation, minimize distribution power losses, relieve heavily loaded feeders, and enhance equipment reliability.⁵ However, inappropriate DGs location and sizing can lead to various negative impacts on the DN, such as voltage instability, increased power losses, harmonic distortion, and even equipment damage, which can affect the reliability and quality of power supply, potentially leading to economic losses and customer dissatisfaction.⁶ Therefore, an optimal operation of the system is necessary to make full use of the benefits of DGs while mitigating their adverse effects.

A considerable amount of research has been conducted on optimal DG integration from various perspectives. In one study, Mansouri et al.⁷ delved into numerous technological challenges that arise from the widespread penetration of PV into DNs, such as active power reduction, frequency regulation, energy storage, and reactive power injection. Another study⁸ explored the technical obstacles that arise due to the extensive and intensive integration of PV into the DNs, such as frequency disturbances and voltage limit violations, as well as the resulting stability issues. The implications of integrating PV on a large scale into the DNs were also

considered, along with potential solutions. The search-based dragonfly algorithm was introduced as a proposed solution for the ideal allocation of DGs, taking into account uncertainties in load demand and DGs. In Prakash and Khatod,⁹ various strategies for locating and sizing DGs in DNs were evaluated. In Zellagui et al.,¹⁰ two popular methods, the particle swarm optimization (PSO) and the firefly method, were proposed as means of achieving operational, financial, and environmental benefits in DNs. In a recent study,¹¹ a combined approach utilizing the PSO and hybrid enhanced gray wolf algorithms was proposed for the optimum location for DGs. This approach aimed to minimize active power losses, system costs, and emissions while improving the voltage stability index (VSI) and reducing the voltage deviation index (VDI). A bioinspired algorithm based on Monte Carlo simulation was proposed by Hemeida et al.¹² In Rathore and Patidar,¹³ the PSO coefficient was employed to minimize total energy losses by optimizing the sizing and deployment of DGs. In El Sehiemy et al.,¹⁴ the Slap swarm optimizer was utilized to enhance the operational, financial, and environmental performance of power plants. The equilibrium optimizer method was introduced by Ahmed et al.¹⁵ A highly effective algorithm was proposed for improving the size and placement of DGs within power networks and addressing the issues with microenergy management. In a study by Thokar et al.,¹⁶ a bilayer approach to the placement of energy storage systems and PV in DNs was proposed. In Biswal and Shankar,¹⁷ the Strength Pareto Evolutionary Algorithm 2 was proposed as a solution for the problem of capacitor and DGs placement with load uncertainty. In Hadidian-Moghaddam et al.,¹⁸ an innovative ant lion optimizer approach was proposed with the goal of lowering energy costs, reducing losses and voltage deviation (VD), and improving reliability. In Ahmed et al.,¹⁹ the PSO approach was proposed, utilizing a probabilistic uncertainty modeling approach, for the siting and sizing of DGs. In Rao et al.,²⁰ Monte Carlo simulation was used for the best placement of DGs within power systems. In this research, Ullah et al.²¹ create an energy optimization framework for intelligent microgrids with the aim of reducing operational expenses, minimizing emissions, and enhancing availability. In Ali et al.,²² a demand side management strategy is proposed to optimize operational cost, pollution emission, and load coordination in smart grid using multi-objective wind-driven optimization and modeling consumer behavior the paper uses probability density function (pdf) to forecast wind speed for integrating wind power. Hafeez et al.²³ propose an energy management strategy using price-based demand response programs in an internet-of-things-enabled smart grid to

schedule smart home appliances. In Hafeez et al.,²⁴ a modular framework for efficient load scheduling in the smart grid, utilizing a hybrid algorithm and real-time pricing data to reduce costs and peak demands, benefiting both residents and power companies.

In Sakr et al.,²⁵ a revised differential evolution algorithm was introduced for the best positioning of DGs. Additionally, the gorilla troops optimizer, which models gorilla social behavior and movement, has been applied to various engineering problems, including PV model extraction.²⁶

The incorporation of the Levy flight distribution has been found to enhance the performance of optimization algorithms for engineering global optimization problems, leading to improved optimal solutions, as demonstrated in several studies.²⁷ Additionally, balancing fitness and distance has been shown to enhance the algorithm's capabilities for searching, as reported in various studies.²⁸ Overall, these findings highlight the potential of incorporating these techniques into optimization algorithms for engineering design problems.

Table 1 lists a comparison between the presented work and other related references for the Optimal Operation problem (OOP) of DNs with RERs.

This research paper proposes a modified version of the Modified Reptile Search Algorithm (MRSA) for the optimal operation of DNs. The proposed approach is compared against several established optimization techniques, including Sand Cat Swarm Optimization

(SCSO),²⁹ PSO,³⁰ Dandelion Optimizer (DO),³¹ Sine Cosine Algorithm (SCA),³² improved harmony search (IHS),³³ and the conventional Reptile Search Algorithm (RSA).²⁸ The study considers the integration of PV and WT generators into DNs with the primary objective of cost minimization and the summation of VD and VSI over a 24-h planning horizon. The model's performance is assessed in the presence of uncertainty in load, wind speed, solar irradiation, temperature, and energy prices for purchasing. Weather data, such as irradiance and temperature, are crucial input variables for simulating PV, whereas the output power of WT is influenced by several factors, such as turbine size and wind speed. Therefore, an accurate modeling approach is essential due to the sensitivity of both PV and WT. To this end, the study employs actual data on irradiance, temperature, and wind speed from the DN area, namely, from the real 112-bus Algerian DN, to guarantee the precision and practicality of the findings.

The novelty and significant contributions of the developed algorithm compared with existing works are articulated as follows:

1. This study proposes an MRSA specifically designed to solve the optimal planning problem involving RERs within DNs.
2. Investigating the synergies between RERs (WTs and PVs), thereby enhancing grid stability and reducing reliance on expensive grid energy purchases.

TABLE 1 Comparison between the presented work and other related references for the Optimal Operation of distribution networks.

Reference	Type of DG	Uncertainty					Improved approach	Objective function	
		Loading	Irradiance	Wind speed	Temperature	Price		Technical	Economical
[10]	PV with DSTATCOM	✓	✓	✗	✗	✗	✗	✓	✓
[11]	PV with capacitors	✗	✗	✗	✗	✗	✓	✓	✓
[12]	WT	✓	✗	✗	✗	✗	✗	✓	✗
[13]	PV + WT + Gravity energy storage	✓	✓	✓	✗	✗	✗	✓	✗
[15]	PV with WT	✓	✓	✗	✗	✗	✗	✓	✓
[16]	PV with energy storage	✓	✓	✗	✗	✗	✗	✓	✗
[17]	PV with capacitors	✓	✗	✗	✗	✗	✗	✓	✓
[18]	PV	✗	✗	✗	✗	✗	✗	✓	✓
[19]	WT	✗	✗	✓	✗	✗	✗	✓	✗
[20]	Conventional DG with WT	✗	✗	✓	✗	✗	✗	✓	✗
This paper	PV with WT	✓	✓	✓	✓	✓	✓	✓	✓

Abbreviations: DG, Distributed Generation; DSTATCOM, distributed static compensator; PV, photovoltaic; WT, wind turbine.

3. The effectiveness and reliability of the MRSA algorithm are rigorously demonstrated through extensive statistical comparisons with established optimization techniques.
4. Rigorous uncertainty analysis to account for the stochastic nature of key parameters, including load demand, solar irradiation, wind speed, temperature, and energy pricing. This facilitates the robust optimization of the distribution grid operation.
5. The proposed MRSA algorithm is tested on standard benchmark functions and applied to address the optimal operation challenges of a real 112-bus Algerian DN.

This paper is organized as follows: In Section 2, the optimal planning problem formulation. Section 3 outlines the modeling approach for uncertainty parameters. Sections 4 and 5 explain the mathematical formulation of the RSA and the proposed MRSA, respectively. Section 6 provides the simulation results. Lastly, the conclusions of this paper are depicted in Section 7.

2 | PROBLEM FORMULATION

This section describes the problem formulation that includes the objective functions and the corresponding constraints of the optimal operation.

2.1 | Objective function

In this paper, three objective functions are considered which include the following:

2.1.1 | Cost minimization

The objective function taken into consideration comprises the cost of electricity acquired from the network (C_{Grid}), the cost of PV units (C_{PV}), the cost of WT (C_{Wind}), and the yearly cost of energy loss (C_{Loss}), and it may be expressed as follows³⁴:

$$C = \min(C_{Grid} + C_{PV} + C_{Wind} + C_{Loss}). \quad (1)$$

In which,

$$C_{Grid} = 365 \times \sum_{h=1}^{24} P_{Grid(h)} \times U_{Grid(h)}, \quad (2)$$

where U_{Grid} represents the cost of purchasing electricity from the grid, and $P_{Grid(h)}$ refers to the power withdrawn from the grid.³⁵

$$C_{Loss} = 365 \times U_{Loss} \times \sum_{h=1}^{24} P_{T_Loss(h)}, \quad (3)$$

where U_{Loss} is the cost of energy, and $P_{T_Loss(h)}$ refers to the total power losses.

$$C_{PV} = C_{PV}^{inst.} + C_{PV}^{O\&M}, \quad (4)$$

where $C_{PV}^{inst.}$ is the cost of installing the PV, $C_{PV}^{O\&M}$ is the PV unit's operating and maintenance costs.³⁴

$$C_{PV}^{O\&M} = U_{PV}^{O\&M} \times \sum_{h=1}^{24} P_{PV(h)}, \quad (5)$$

$$C_{PV}^{inst.} = CF \times U_{PV} \times P_{rated_PV}, \quad (6)$$

where CF is a factor affecting capital recovery, P_{rated_PV} is the rated produced power of the PV.³⁴

$$C_{Wind} = C_{wind}^{inst.} + C_{wind}^{O\&M}, \quad (7)$$

where $C_{Wind}^{inst.}$ is the cost of installing the WT, and $C_{wind}^{O\&M}$ is the wind's operating and maintenance costs.³⁴

$$C_{Wind}^{O\&M} = U_{Wind}^{O\&M} \times \sum_{h=1}^{24} P_{Wind(h)}, \quad (8)$$

where $U_{PV}^{O\&M}$ and $U_{Wind}^{O\&M}$ represent the WTs and PVs operation and maintenance costs (\$/kW).³⁴

$$C_{Wind}^{inst.} = CF \times U_{WT} \times P_{rated_wind}, \quad (9)$$

where P_{rated_wind} is the rated produced power of WT, U_{WT} and U_{PV} represent the WTs and PVs purchased cost (\$/kW), and $P_{Wind(h)}$ and $P_{PV(h)}$ represent the yielded power from WTs and PVs systems.

$$CF = \frac{\beta \times (1 + \beta)^{NP}}{(1 + \beta)^{NP} - 1}, \quad (10)$$

where β and NP the interest rate and system lifetime of the winds turbine or PV unit.³⁶

The generated power from the PV can be calculated as follows:

$$T_c = T_a + \frac{I_s}{800} \cdot (T_N - 20), \quad (11)$$

$$P_{pv}(t) = A_{pv} \cdot \eta_{pv}(t) \cdot I(t). \quad (12)$$

The surface area utilized by the set of PV, denoted as A_{pv} in (m²), is multiplied by a constant value

representing the conversion efficiency of the PV panels, for the purpose of calculating the power generated by the PV, denoted as P_{pv} (kW), I solar insolation in (kW/m^2) and η_{pv} represent the instantaneous efficiency of PV panels. The instantaneous efficiency of PV panels is obtained using the following equation³⁷:

$$\begin{aligned} \eta_{pv}(t) &= \eta_r \cdot \eta_t \\ &\times \left[1 - \beta \cdot (T_a(t) - T_r) \right. \\ &\quad \left. - \beta \cdot I(t) \cdot \left(\frac{NOCT - 20}{800} \right) \cdot \right. \\ &\quad \left. (1 - \eta_r \cdot \eta_t) \right]. \end{aligned} \quad (13)$$

The effectiveness of the maximum power point tracking equipment is denoted by η_t , and η_r represents the reference efficiency of the PV panels. The temperature coefficient of efficiency β , typically ranging from 0.004 to 0.006/ $^{\circ}\text{C}$ for silicon cells, is also considered. The ambient temperature T_a ($^{\circ}\text{C}$), PV cell reference temperature T_r ($^{\circ}\text{C}$), and nominal operating cell temperature $NOCT$ ($^{\circ}\text{C}$) are also taken into account.

The WT's produced output power (P_{WT}) is computed as follows:

$$\begin{aligned} P_{WT}(W) &= \begin{cases} 0 & \text{for } W < W_i \text{ and } W > W_o, \\ P_{rated_wind} \left(\frac{W - W_i}{W_r - W_i} \right) & \text{for } (W_i \leq W \leq W_r), \\ P_{rated_wind} & \text{for } (W_r < W \leq W_o), \end{cases} \end{aligned} \quad (14)$$

the rated power of the used WT is 250 kW while its rated velocity (W_r) is 15 m/s, the cut-in speed (W_i) is 2.5 m/s, and cut-out speed (W_o) the WT taken as 25 m/s.³⁸

2.1.2 | Enhancement of voltage level

To improve the network performance, the voltage deviations should be kept closed to 1 p.u. value which can be defined as^{36,39}

$$\sum VD = \sum_{h=1}^{24} \sum_{k=1}^{NB} |(V_k - 1)|, \quad (15)$$

where NB represents the number of buses in the network, and V_k represents the voltage of the k th bus.

2.1.3 | Improved system stability

The system stability index statement is as follows^{40,41}:

$$\begin{aligned} VSI_k &= |V_k|^4 - 4(P_k X_{km} - Q_k R_{km})^2 \\ &\quad - 4(P_k X_{km} + Q_k R_{km}) |V_k|^2, \end{aligned} \quad (16)$$

$$\sum VSI = \sum_{h=1}^{24} \sum_{k=1}^{NB} VSI_k, \quad (17)$$

where VSI_k is the voltage stability index, R_{km} represent the resistance of the transmission lines while the X_{km} is its reactance. P_k and Q_k define the real and reactive power at bus, respectively. The following three objective functions are taken into consideration simultaneously:

$$F = \varepsilon_1 F_1 + \varepsilon_2 F_2 + \varepsilon_3 F_3, \quad (18)$$

$$F_1 = \frac{C_{RERS}}{C_{Base}}, \quad (19)$$

$$F_2 = \frac{\sum VD_{RERS}}{\sum VD_{Base}}, \quad (20)$$

$$F_3 = \frac{1}{\sum VSI_{RERS}}, \quad (21)$$

where $RERS$ and $Base$ are subscripts refers to with RERS and the base case, respectively. ε_1 , ε_2 , and ε_3 are the weighted factors that were selected to be 0.5, 0.25, and 0.25, respectively.⁴²

2.2 | Limitations of the network

$$V_{Min} \leq V_i \leq V_{Max}, \quad (22)$$

$$P_{PV_rated} + P_{wind_rated} \leq \sum_{i=1}^{NB} P_{Load,i}, \quad (23)$$

$$PF_{Min} \leq PF \leq PF_{Max}, \quad (24)$$

$$I_n \leq I_{max,n}, \quad n = 1, 2, 3, \dots, NT, \quad (25)$$

where V_{min} and V_{max} are the lower and upper voltage limits. P_{Load} and Q_{Load} signified the real and reactive load, respectively; $I_{max,n}$ is the maximum allowable current limit of the line; NT defines the number of lines; PF_{max} and PF_{min} are the maximum and minimum of the WT power factor, respectively.

2.2.1 | Equality constraints

$$P_S + P_{PV} + P_{Wind} = \sum_{i=1}^{NT} P_{Loss,i} + \sum_{i=1}^{NB} P_{Load,i}, \quad (26)$$

$$Q_S + Q_{Wind} = \sum_{i=1}^{NT} Q_{Loss,i} + \sum_{i=1}^{NB} Q_{Load,i}, \quad (27)$$

where Q_S and P_S are the reactive and real powers of the main network.

3 | MODELING THE UNCERTAINTIES

In this section, the considered uncertain parameters are represented as follows:

3.1 | The probabilistic model of solar irradiance

The Beta pdf has been employed to model the intermittent nature of the solar irradiance, as follows^{43,44}:

$$f(g_s) = \begin{cases} \frac{\Gamma(\alpha + \beta)}{\Gamma(\alpha)\Gamma(\beta)} s^{\alpha-1} (1 - g_s)^{\beta-1}, & 0 \leq g_s \leq 1, \alpha, \beta \geq 0, \\ 0, & \text{otherwise,} \end{cases} \quad (28)$$

where σ is the standard deviation while μ is the mean value which has been obtained from the historical data. β and α can be obtained from the following equations^{45,46}:

$$\beta = (1 - \mu) \times \left(\frac{\mu \times (1 + \mu)}{\sigma^2} - 1 \right), \quad (29)$$

$$\alpha = \frac{\mu \times \beta}{1 - \mu}. \quad (30)$$

3.2 | The probabilistic model of wind speed

For modeling the wind speed uncertainty, the Weibull pdf is utilized which can be described as follows^{47,48}:

$$f(W) = \left(\frac{k}{c} \right) \left(\frac{W}{c} \right)^{k-1} \exp \left[- \left(\frac{W}{c} \right)^k \right], \quad (31)$$

where W represents the wind speed. c and k are the scale and shape parameters of the Weibull pdf.

3.3 | The probabilistic model of load demand

Normal pdf is employed to model the demanding uncertainty that can be mathematically described as follows⁴⁶:

$$f(L) = \frac{1}{\sigma_l \sqrt{2\pi}} \times \exp \left[- \left(\frac{l - \mu_l}{2\sigma_l^2} \right)^2 \right], \quad (32)$$

where σ_l and μ_l are the standard deviation and the mean value of the loading, respectively. The probability of the loading is divided into subsegments according to the following equation:

3.4 | The probabilistic model of price

One of the most significant random characteristics in power systems is the price of electricity, which is an unreliable parameter that is acquired from the grid. To model the probability distribution of the electricity price, the Normal pdf can be used based on its mean value μ_{EP} and standard deviation σ_{EP} , as shown in Equation (33)⁴⁹:

$$f(P) = \frac{1}{\sigma_{EP} \sqrt{2\pi}} \exp \left[- \frac{(EP - \mu_{EP})^2}{2(\sigma_{EP})^2} \right]. \quad (33)$$

3.5 | The probabilistic model of temperature

As the surrounding temperature varies continuously. Thus, the temperature is considered as uncertain parameter and it is assumed that the uncertainty of the temperature is represented using the normal probability distribution for modeling the uncertainty of the temperature as follows:

$$f(T) = \frac{1}{\sqrt{2\pi}\sigma_T} \exp \left[- \frac{(s - \mu_T^t)^2}{2(\sigma_T^t)^2} \right], \quad (34)$$

where σ_T is the standard deviation while μ_T is the mean value of temperature.

4 | REPTILE SEARCH ALGORITHM

The RSA draws inspiration from the hunting and encircling behaviors of crocodiles in the wild. These behaviors involve crocodiles working together to surround and capture their prey.²⁸

RSA uses mathematical modeling to mimic these behaviors and create an optimization process that is both gradient-free and population-based. This means that it can tackle optimization challenges of varying complexities, with or without specific constraints.

4.1 | Initialization phase

RSA begins the optimization by generating a set of possible solutions, represented as X in Equation (35), through a stochastic approach. The algorithm then

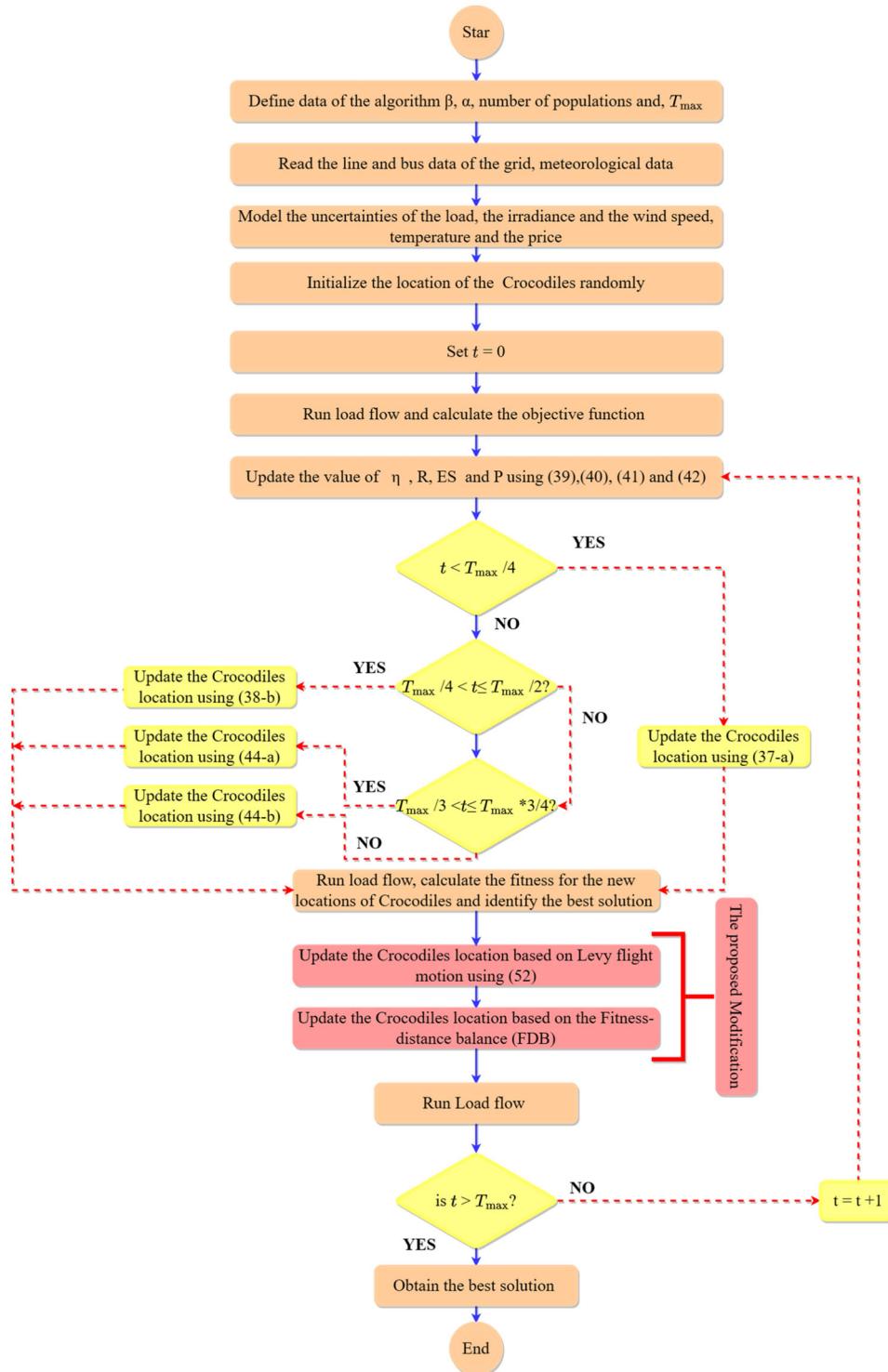


FIGURE 1 Flowchart of the proposed MRSA for optimal operation. MRSA, Modified Reptile Search Algorithm.

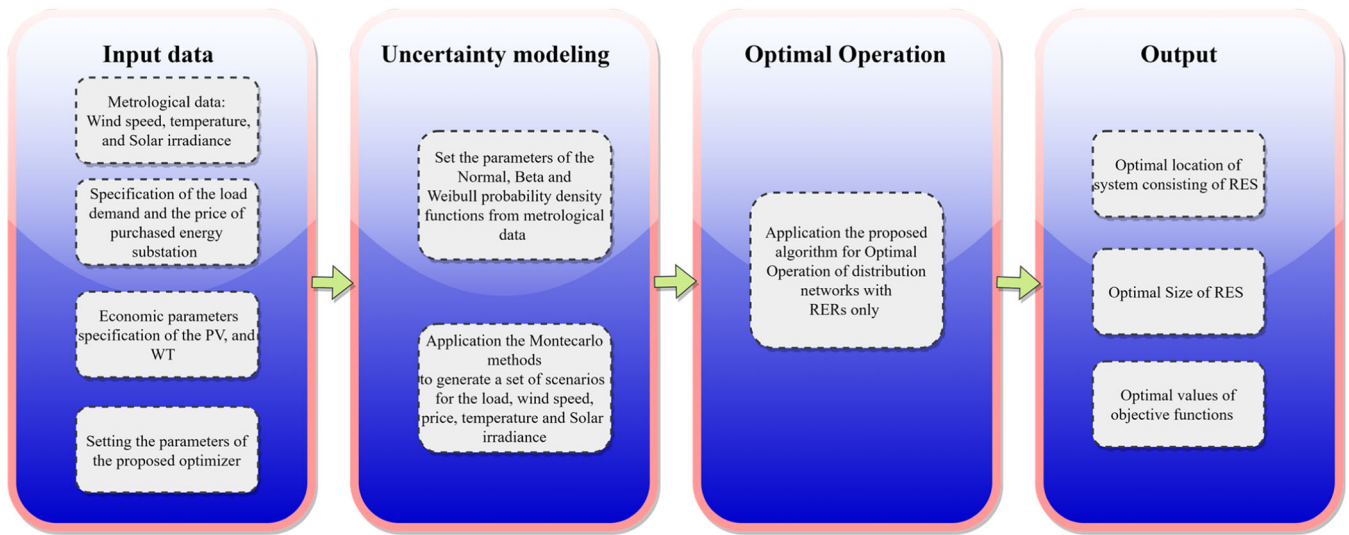


FIGURE 2 Steps procedure for solving the Operation of a Distribution Grid Considering RESs Integration. PV, photovoltaic; RESs, renewable energy sources; WT, wind turbine.

TABLE 2 Selected parameters of the optimizers.

Algorithm	Parameter	Value
SCSO ²⁹	Sensitivity range (<i>rg</i>)	[2, 0]
	Phases control range (<i>R</i>)	[-2 <i>rg</i> , 2 <i>rg</i>]
PSO ³⁰	<i>C</i> 1	2
	<i>C</i> 2	2
	<i>V</i> max	6
DO ³¹	<i>a</i>	[0, 1]
	<i>K</i>	[0, 1]
SCA ³²	<i>a</i>	2
IHS ³³	<i>HMCR</i>	0.95
	<i>PAR</i>	0.45
RSA ²⁸	<i>a</i>	0.1
	<i>β</i>	0.1
MRSA	<i>a</i>	0.1
	<i>β</i>	0.1

Abbreviations: DO, Dandelion Optimizer; HMCR, harmony memory considering rate; IHS, improved harmony search; MRSA, Modified Reptile Search Algorithm; PAR, pitch adjusting rate; PSO, particle swarm optimization; RSA, Reptile Search Algorithm; SCA, Sine Cosine Algorithm; SCSO, Sand Cat Swarm Optimization.

identifies the best solution obtained and considers it as an approximation of the optimal solution in each iteration.

$$X = \begin{bmatrix} x_{1,1} & \cdots & x_{1,j} & x_{1,n-1} & x_{1,n} \\ x_{2,1} & \cdots & x_{2,j} & \cdots & x_{2,n} \\ \cdots & \cdots & x_{i,j} & \cdots & \cdots \\ \vdots & \vdots & \vdots & \vdots & \vdots \\ x_{N-1,1} & \cdots & x_{N-1,j} & \cdots & x_{N-1,n} \\ x_{N,1} & \cdots & x_{N,j} & x_{N,n-1} & x_{N,n} \end{bmatrix} \quad (35)$$

The set of candidate solutions, *X*, used in the RSA is generated randomly through the use of Equation (36), *x_{i,j}* represents the value of the solution at the *j*th position within the *i*th candidate solution. The number of candidate solutions generated is denoted as *N*, while the dimension size of the problem is represented by *n*.

$$x_{ij} = rand \times (UB - LB) + LB, \quad j = 1, 2, \dots, n. \quad (36)$$

4.2 | Exploration phase

Two exploration search methods are utilized in the RSA. Each component is given a stochastic scaling factor to get more varied solutions and investigate different locations. The position-updating equations used in the exploration phase are designed to imitate the surrounding behavior of crocodiles and are presented in Equation (37). It is noteworthy that the algorithm employs a simple rule to facilitate this behavior.

$$x_{(i,j)}(t + 1) = \begin{cases} Best_j(t) \times -\eta_{(i,j)}(t) & t \leq \frac{T}{4}, \\ \times \beta - R_{(i,j)}(t) \\ \times rand, \\ Best(t) \times x_{(r_1,j)} & t \leq \frac{T}{4} \text{ and } t > \frac{T}{4}. \\ \times ES(t) \times rand, \end{cases} \quad (37)$$

The values used in this calculation include *Best_j(t)*, which denotes the position of the *j*th element in the optimal solution obtained until the current point. The

TABLE 3 Statistical results of different optimizers for the standard functions.

Function	Algorithms	Average	Best	Worst	SD	p Value
F1	SCSO	1.38E – 63	4.10E – 75	3.45E – 62	6.89E – 63	9.73E – 11
	PSO	6.424440	3.405028	11.52595	2.484545	9.73E – 11
	DO	0.000996	1.62E – 04	0.005010	0.000943	9.73E – 11
	SCA	182.7205	3.475340	1032.703	255.0227	9.73E – 11
	IHS	3709.594	2534.045	5222.689	765.3992	9.73E – 11
	RSA	0	0	0	0	–
	MRSA	0	0	0	0	9.73E – 11
F2	SCSO	3.87E – 36	1.40E – 39	2.88E – 35	6.98E – 36	9.73E – 11
	PSO	14.61081	5.433588	29.35110	7.175295	9.73E – 11
	DO	0.011470	5.39E – 03	0.020483	0.003692	9.73E – 11
	SCA	0.272542	0.008164	1.280333	0.335631	9.73E – 11
	IHS	12.84327	9.376357	15.42907	1.559890	9.73E – 11
	RSA	0	0	0	0	–
	MRSA	0	0	0	0	9.73E – 11
F3	SCSO	2.86E – 58	2.33E – 67	2.55E – 57	7.48E – 58	9.73E – 11
	PSO	356.9342	172.4677	840.5712	160.1756	9.73E – 11
	DO	199.8629	4.51E + 01	994.6379	197.4348	9.73E – 11
	SCA	13410.65	3860.001	29541.4	7336.314	9.73E – 11
	IHS	34383.79	26383.11	46825.71	5633.336	9.73E – 11
	RSA	0	0	0	0	–
	MRSA	0	0	0	0	9.73E – 11
F4	SCSO	1.39E – 28	9.23E – 34	2.89E – 27	5.77E – 28	9.73E – 11
	PSO	2.489528	1.948191	3.315541	0.324898	9.73E – 11
	DO	3.72332	3.53E – 01	20.19588	3.837033	9.73E – 11
	SCA	46.81593	22.09118	60.92903	11.30440	9.73E – 11
	IHS	40.34242	36.98943	42.37694	1.410474	9.73E – 11
	RSA	0	0	0	0	–
	F5	SCSO	2.82E + 01	2.58E + 01	2.89E + 01	8.22E – 01
PSO		2803.884	1143.793	6242.928	1334.683	1.42E – 09
DO		43.58443	2.41E + 01	208.2927	46.0841	2.78E – 05
SCA		223133.4	1850.487	1938306	426164.4	1.42E – 09
IHS		1989223	927233.6	3433610	634165.5	1.42E – 09
RSA		20.60125	1.83E – 14	29	12.80898	0.028655
MRSA		26.98798	26.08742	27.88721	0.516893	1.12E – 6
F6	SCSO	2.19E + 000	1.24E + 000	3.54E + 000	6.10E – 01	2.29E – 09
	PSO	7.522896	3.574887	12.91259	2.289411	1.42E – 09
	DO	0.000271	6.50E – 05	0.000602	0.000133	1.42E – 09
	SCA	128.2935	8.85283	744.3154	156.7731	1.42E – 09
	IHS	3526.831	2250.587	4877.084	723.5816	1.42E – 09

(Continues)

TABLE 3 (Continued)

Function	Algorithms	Average	Best	Worst	SD	p Value
F7	RSA	7.331290	5.710000	7.5	0.381222	6.58E – 10
	MRSA	0.608169	0.218609	1.415836	0.257723	2.29E – 09
	SCSO	3.08E – 04	8.55E – 06	3.10E – 03	6.10E – 04	0.000331
	PSO	10.78179	1.576448	46.78055	9.612627	1.42E – 09
	DO	0.035633	1.67E – 02	0.068770	0.014530	1.42E – 09
	SCA	0.260816	0.021967	0.894358	0.269184	1.42E – 09
	IHS	1.290274	0.854433	2.013562	0.282050	1.42E – 09
	MRSA	7.63E – 05	1.48E – 06	0.000403	9.56E – 05	0.000331
F8	SCSO	–6.40E + 03	–7.83E + 03	–5.03E + 03	7.72E + 02	2.29E – 09
	PSO	–5620.21	–8082.7	–3130.020	1426.450	1.80E – 09
	DO	–7665.32	–8.56E + 03	–6053.18	547.5695	6.89E – 08
	SCA	–3662.45	–4422.04	–3206.05	300.7578	1.42E – 09
	IHS	–11322.6	–11687.2	–10999	164.3765	5.62E – 06
	RSA	–4990.86	–5.64E + 03	–3377.24	705.1705	1.41E – 09
	MRSA	–1.00E + 04	–1.25E + 04	–7326.62	1.23E + 03	2.29E – 09
	F9	SCSO	0.000E + 000	0.000E + 000	0.000E + 000	0.000E + 000
PSO		250.6723	190.465	306.2746	34.95964	9.73E – 11
DO		36.71142	5.10E + 000	106.8397	24.08433	9.73E – 11
SCA		71.89162	14.4388	187.1399	44.45624	9.73E – 11
IHS		63.91474	52.07516	77.19766	7.126956	9.73E – 11
RSA		0	0	0	0	N/A
MRSA		0	0	0	0	–
F10		SCSO	8.88E – 16	8.88E – 16	8.88E – 16	0.00E + 000
	PSO	3.51132	2.417290	4.259182	0.422709	9.73E – 11
	DO	0.00799	3.18E – 03	0.012885	0.002006	9.73E – 11
	SCA	14.51416	0.624838	20.36937	8.212028	9.73E – 11
	IHS	11.45441	10.32844	12.78042	0.622297	9.73E – 11
	RSA	8.888E – 16	8.888E – 16	8.888E – 16	0	N/A
	MRSA	8.888E – 16	8.888E – 16	8.888E – 16	0	–
	F11	SCSO	0	0	0	0
PSO		0.376341	0.241846	0.581791	0.098999	9.73E – 11
DO		0.014719	6.15E – 04	0.063421	0.016309	9.73E – 11
SCA		2.079527	0.514695	5.884849	1.452231	9.73E – 11
IHS		33.42945	22.37086	47.96473	6.541254	9.73E – 11
RSA		0	0	0	0	–
MRSA		0	0	0	0	–

TABLE 3 (Continued)

Function	Algorithms	Average	Best	Worst	SD	p Value
F12	SCSO	1.28E – 01	6.07E – 02	3.08E – 01	5.96E – 02	1.42E – 09
	PSO	0.223935	0.035205	0.701546	0.165885	2.29E – 09
	DO	0.126405	3.95E – 06	1.155118	0.308977	0.029771
	SCA	3065855	2.741164	37929699	8385062	1.42E – 09
	IHS	248120.3	19626.86	660950.4	145754.7	1.42E – 09
	RSA	1.52E + 000	7.65E – 01	1.67E + 000	0.293867	5.66E – 10
	MRSA	2.10E – 02	5.74E – 03	5.09E – 02	1.17E – 02	1.42E – 09
F13	SCSO	2.46E + 000	1.28E + 000	2.89E + 000	4.26E – 01	1.42E – 09
	PSO	1.582987	0.951961	2.47593	0.461503	1.42E – 09
	DO	0.00504	5.88E – 05	0.021212	0.006323	1.42E – 09
	SCA	2995027	215.1451	55398050	11004997	1.42E – 09
	IHS	2998273	458341.9	5990629	1293964	1.42E – 09
	RSA	7.49E – 01	4.26E – 18	3.00E + 000	1.236653	1.40E – 09
	MRSA	1.23E – 26	8.62E – 32	1.73E – 25	3.72E – 26	1.42E – 09
F14	SCSO	3.71E + 000	9.98E – 01	1.08E + 01	3.28E + 000	1.70E – 05
	PSO	3.835392	0.998004	7.873993	2.756515	0.000546
	DO	1.037765	9.98E – 01	1.992031	0.198805	0.001539
	SCA	2.04507	0.998004	2.982105	0.996002	8.53E – 05
	IHS	0.998011	0.998004	0.998186	3.65E – 05	0.001542
	RSA	4.18E + 000	1.03E + 000	1.27E + 01	3.108389	6.93E – 06
	MRSA	2.56E + 000	9.98E – 01	1.27E + 01	3.64E + 000	1.70E – 05
F15	SCSO	5.51E – 04	3.07E – 04	1.22E – 03	3.19E – 04	4.46E – 08
	PSO	0.008475	0.000753	0.022553	0.009408	1.42E – 09
	DO	0.002152	3.08E – 04	0.020363	0.005487	6.57E – 09
	SCA	0.001163	0.000723	0.001636	0.000343	1.42E – 09
	IHS	0.002797	0.000625	0.021701	4.21E – 03	1.42E – 09
	RSA	2.80E – 03	7.72E – 04	7.24E – 03	0.00202	1.42E – 09
	MRSA	3.08E – 04	3.08E – 04	3.18E – 04	2.66E – 06	4.46E – 08
F16	SCSO	–1.030E + 000	–1.030E + 000	–1.030E + 000	1.13E – 09	0.472337
	PSO	–1.03163	–1.03163	–1.03163	7.93E – 14	0.185999
	DO	–1.03163	–1.03E + 000	–1.03163	7.18E – 12	0.228482
	SCA	–1.03156	–1.03163	–1.03143	5.07E – 05	1.95E – 09
	IHS	–1.03115	–1.03163	–1.02957	5.51E – 04	1.36E – 09
	RSA	–1.030E + 000	–1.030E + 000	–1.030E + 000	0.001163	1.36E – 09
	MRSA	–1.030E + 000	–1.030E + 000	–1.030E + 000	3.58E – 08	0.472337
F17	SCSO	3.98E – 01	3.98E – 01	3.98E – 01	1.24E – 07	9.73E – 11
	PSO	0.397887	0.397887	0.397887	1.21E – 14	0.001164
	DO	0.397887	3.98E – 01	0.397887	2.09E – 10	9.73E – 11
	SCA	0.400606	0.397888	0.406122	2.57E – 03	9.73E – 11

(Continues)

TABLE 3 (Continued)

Function	Algorithms	Average	Best	Worst	SD	p Value
	IHS	0.398056	0.397891	0.398643	1.67E – 04	9.73E – 11
	RSA	4.45E – 01	3.99E – 01	6.15E – 01	0.051209	9.73E – 11
	MRSA	3.988E – 01	3.988E – 01	3.988E – 01	0	9.73E – 11
F18	SCSO	3.000E + 000	3.000E + 000	3.000E + 000	2.21E – 05	1.35E – 09
	PSO	3	3	3	9.70E – 13	1.35E – 09
	DO	3	3.00E + 000	3	5.10E – 08	1.35E – 09
	SCA	3.000244	3.000004	3.001866	4.04E – 04	1.35E – 09
	IHS	3.004249	3.000239	3.017577	5.11E – 03	1.35E – 09
	RSA	6.47E + 000	3.00E + 000	3.28E + 01	9.552113	1.35E – 09
	MRSA	3.00E + 000	3.00E + 000	3.00E + 000	3.21E – 15	1.35E – 09
F19	SCSO	–3.860E + 000	–3.860E + 000	–3.860E + 000	8.49E – 05	0.007937
	PSO	–3.86278	–3.86278	–3.86278	2.34E – 13	0.007937
	DO	–3.86278	–3.86E + 000	–3.86278	2.67E – 07	0.007937
	SCA	–3.8534	–3.85836	–3.85082	3.11E – 03	0.007937
	IHS	–3.86274	–3.86277	–3.86272	2.03E – 05	0.007937
	RSA	–3.790E + 000	–3.810E + 000	–3.780E + 000	0.011682	0.007937
	MRSA	–3.860E + 000	–3.860E + 000	–3.860E + 000	4.97E – 16	0.007937
F20	SCSO	–3.200E + 000	–3.320E + 000	–2.430E + 000	1.79E – 01	0.013733
	PSO	–3.13442	–3.322	–1.70606	3.38E – 01	0.091402
	DO	–3.25541	–3.32E + 000	–3.20301	6.02E – 02	0.252305
	SCA	–2.8142	–3.24815	–1.4431	5.41E – 01	1.17E – 08
	IHS	–3.30751	–3.32196	–3.20226	3.95E – 02	0.084194
	RSA	–2.48	–3.02	–1.33	0.423885	1.42E – 09
	MRSA	–3.23	–3.32	–3.14	6.05E – 02	0.013733
F21	SCSO	–5.21E + 000	–1.02E + 01	–8.82E – 01	2.16E + 000	1.41E – 09
	PSO	–7.65757	–10.1532	–2.63047	3.22E + 000	1.41E – 09
	DO	–6.22932	–1.02E + 01	–2.63047	3.16E + 000	1.41E – 09
	SCA	–2.09573	–5.55252	–0.49724	1.76E + 000	1.41E – 09
	IHS	–4.75303	–10.1504	–2.62343	3.42E + 000	1.41E – 09
	RSA	–5.06E + 000	–5.06E + 000	–5.06E + 000	4.53E – 07	1.41E – 09
	MRSA	–1.02E + 010	–1.02E + 010	–1.02E + 010	2.21E – 10	1.41E – 09
F22	SCSO	–6.13E + 000	–1.04E + 01	–9.10E – 01	2.92E + 000	1.42E – 09
	PSO	–7.35997	–10.4029	–1.83759	3.44E + 000	1.42E – 09
	DO	–6.25978	–1.04E + 01	–1.83759	3.80E + 000	1.42E – 09
	SCA	–3.35866	–6.91684	–0.90076	1.72E + 000	1.42E – 09
	IHS	–6.68595	–10.4026	–2.75128	3.64E + 000	1.42E – 09
	RSA	–5.04E + 000	–5.09E + 000	–3.80E + 000	2.58E – 01	1.42E – 09
	MRSA	–1.04E + 01	–1.04E + 01	–1.04E + 01	8.37E – 11	1.42E – 09

TABLE 3 (Continued)

Function	Algorithms	Average	Best	Worst	SD	p Value
F23	SCSO	-5.86	-1.05E + 01	-1.68	2.20E + 000	6.25E + 00
	PSO	-8.75315	-10.5364	-2.42173	3.04E + 000	1.67E + 00
	DO	-5.12039	-1.05E + 01	-1.85948	3.24E + 000	8.04E + 00
	SCA	-3.39436	-7.4654	-0.93762	2.15E + 000	2.21E + 00
	IHS	-6.26178	-10.535	-2.42036	3.87E + 000	1.16E + 01
	RSA	-5.130	-5.130	-5.130	1.78E - 06	1.02E + 01
	MRSA	-1.050E + 010	-1.050E + 010	-1.050E + 010	3.68E - 10	2.53E + 01

Note: Bold values indicate the best obtained solutions.

Abbreviations: DO, Dandelion Optimizer; IHS, improved harmony search; MRSA, Modified Reptile Search Algorithm; PSO, particle swarm optimization; RSA, Reptile Search Algorithm; SCA, Sine Cosine Algorithm; SCSO, Sand Cat Swarm Optimization.

integer $rand$ is created at random and ranges from 0 to 1, T , the upper limit of iterations and t , the current iteration number. Equation (38) is used to calculate the hunting operator, denoted as (i, j) , for the j th location in the i th solution. Iterations are conducted with a fixed sensitive parameter, β , set to 0.1, to regulate the exploration accuracy during the encircling phase. A reduction function, denoted as $R_{(i,j)}$, is employed to narrow down the search area and its calculation is determined by Equation (39). The random number r_1 , generated between $[1 N]$, is used to represent a stochastic location in the i th solution, represented by $x_{(r_1,j)}$. The value of N represents the number of candidate solutions. The Evolutionary Sense $ES(t)$ probability ratio varies randomly between 2 and -2 during each iteration according to Equation (40).

$$\eta_{(i,j)} = Best_j(t) \times P_{(i,j)}, \quad (38)$$

$$R_{(i,j)} = \frac{Best_j(t) - x_{(r_2,j)}}{Best_j(t) + \epsilon}, \quad (39)$$

$$ES(t) = 2 \times r_3 \times \left(1 - \frac{1}{T}\right). \quad (40)$$

This equation describes some variables used in RSA, including r_2 , which is a random number between $[1 N]$, and ϵ , which is a small value. The equation also involves the use of r_3 , which represents a random value among -1 and 1 . $P_{(i,j)}$ is another variable used in the algorithm, which represents the proportional difference between of the j th position of the best-obtained solution and the j th position of the current solution. This calculation is performed using Equation (41).

$$P_{(i,j)} = \alpha + \frac{x_{(i,j)} - M(x_i)}{Best_j(t) \times (UB_{(j)} - LB_{(j)}) + \epsilon}. \quad (41)$$

This excerpt explains the variables used in the hunting cooperation phase. The average position of the current solution is denoted by $M(x_i)$, which is calculated using Equation (41). $UB_{(j)}$ and $LB_{(j)}$ represent the upper and lower boundaries of the j th position, respectively. The parameter α is fixed at 0.1 in this study.

$$M(x_i) = \frac{1}{n} \sum_{j=1}^n x_{(i,j)}. \quad (42)$$

4.3 | Exploitation phase

The RSA algorithm uses two main search strategies, namely, hunting cooperation and hunting coordination, to investigate the search space and locate an ideal solution. These strategies are modeled in Equation (43) and are used for exploitation mechanisms.

$$x_{(i,j)}(t+1) = \begin{cases} Best_j(t) \times P_{(i,j)}(t) & t \leq 3\frac{T}{4} \text{ and } t > 2\frac{T}{4} \\ \times rand, & \\ Best_j(t) - \eta_{(i,j)}(t) & t \leq T \text{ and } t > 3\frac{T}{4}, \\ \times \epsilon - R_{(i,j)}(t) & \\ \times rand. & \end{cases} \quad (43)$$

The j th location in the optimal solution obtained until now is represented by the term $Best_j(t)$. The hunting operator applied to j th location in the i th solution, denoted as $\eta_{(i,j)}$, is calculated using Equation (38). The disparity

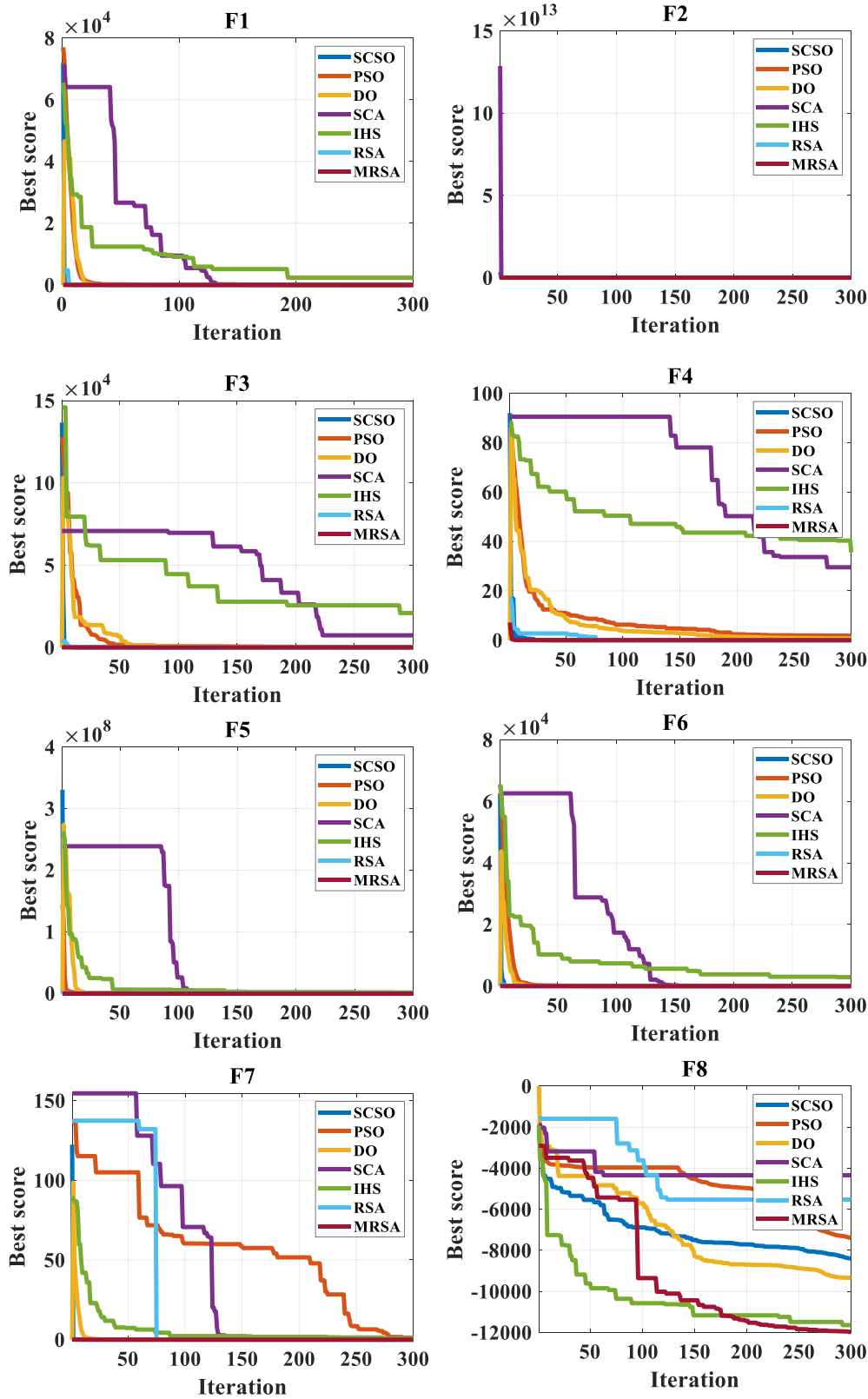


FIGURE 3 Convergence curves of the test benchmark functions by different optimizers. DO, Dandelion Optimizer; IHS, improved harmony search; MRSA, Modified Reptile Search Algorithm; PSO, particle swarm optimization; RSA, Reptile Search Algorithm; SCA, Sine Cosine Algorithm; SCSO, Sand Cat Swarm Optimization.

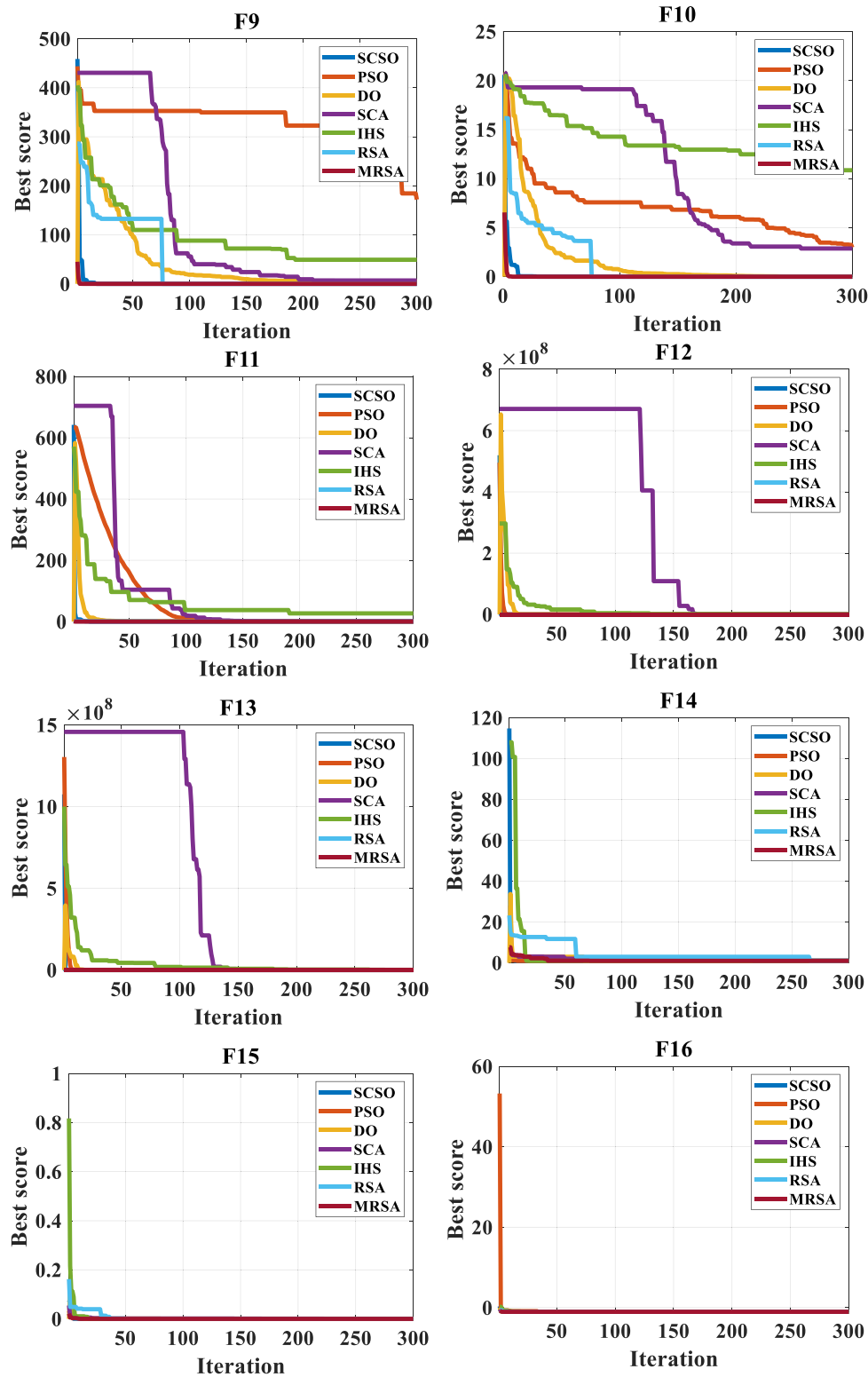


FIGURE 3 (Continued).

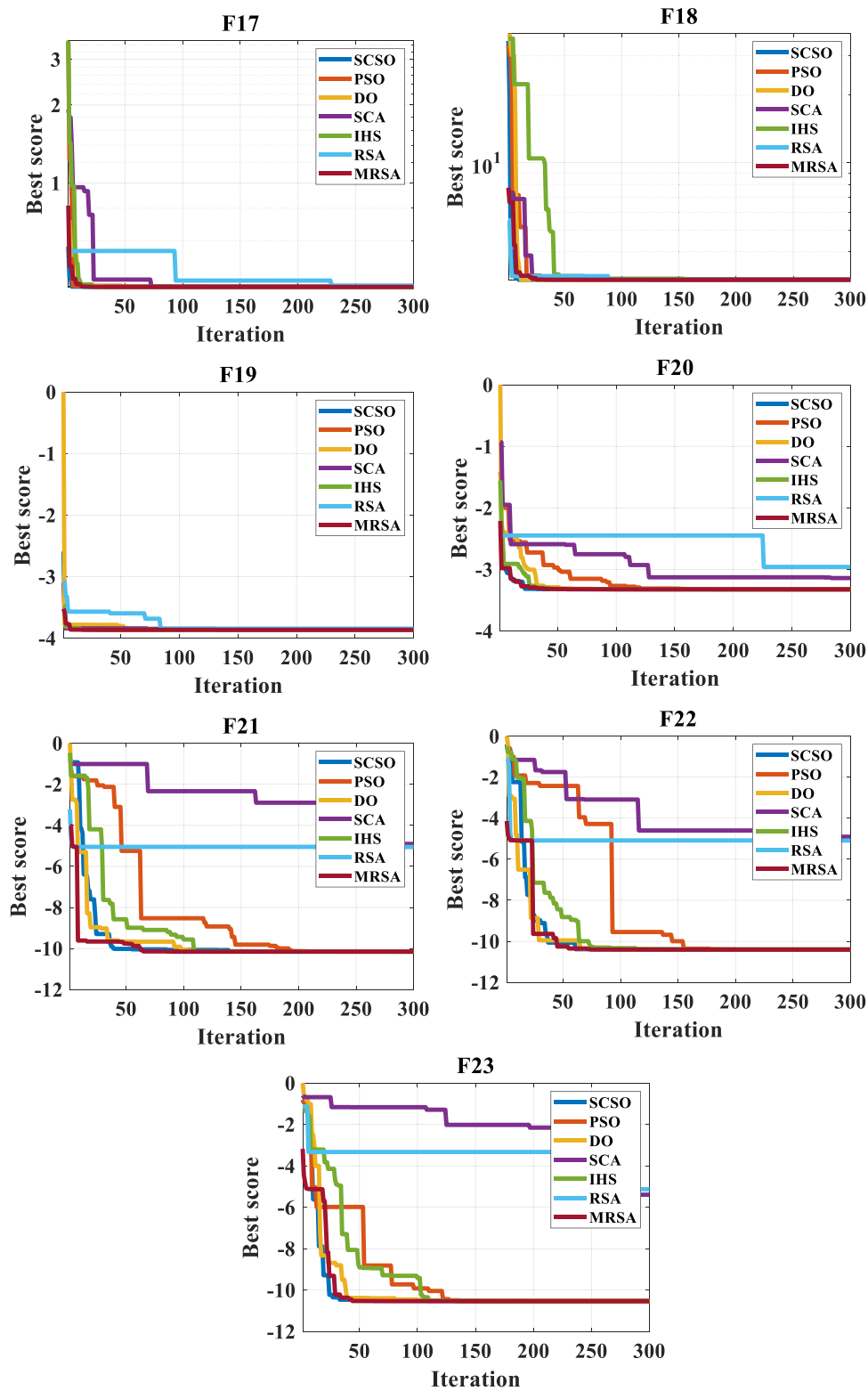


FIGURE 3 (Continued).

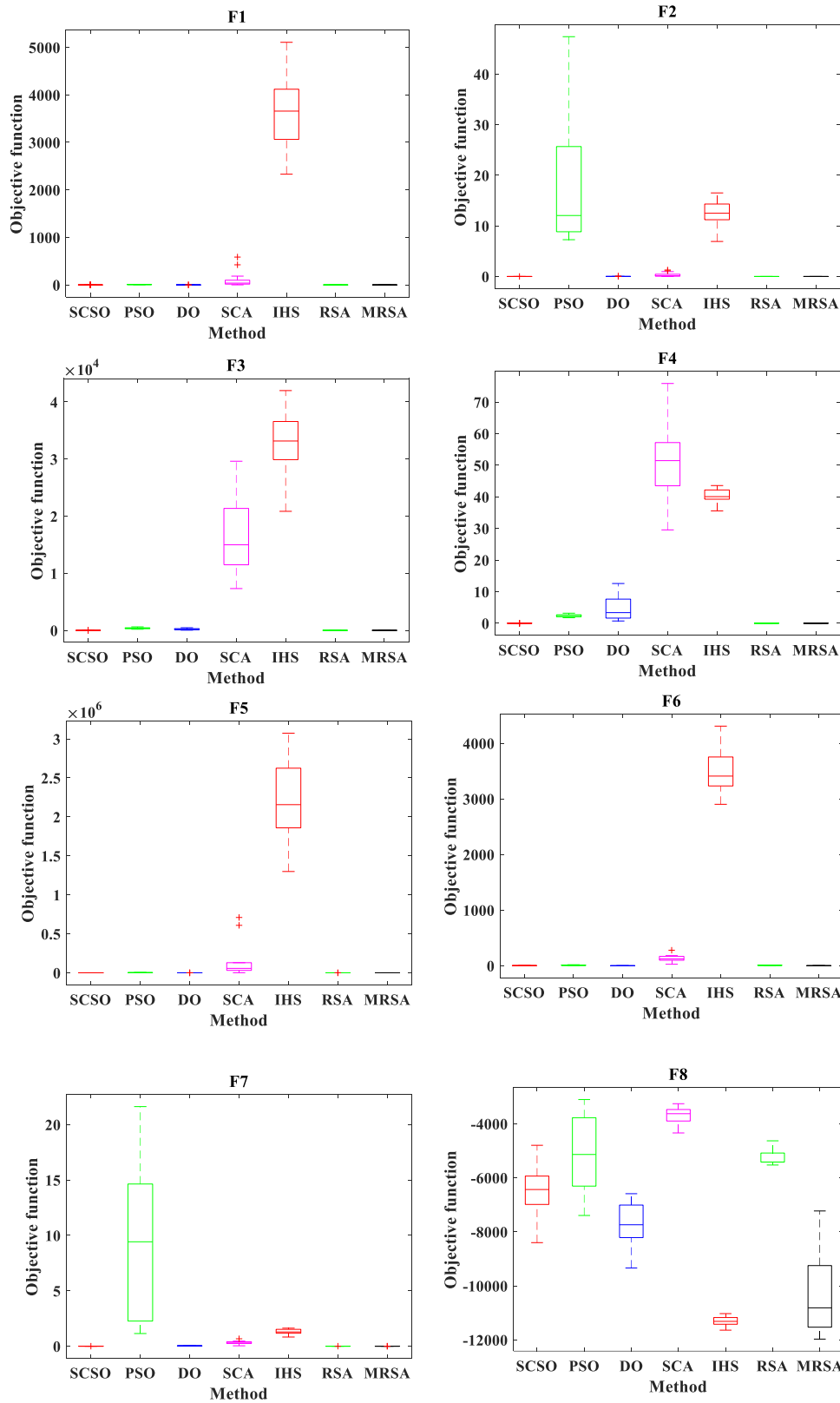


FIGURE 4 Boxplot for test benchmark functions by different optimizers. DO, Dandelion Optimizer; IHS, improved harmony search; MRSA, Modified Reptile Search Algorithm; PSO, particle swarm optimization; RSA, Reptile Search Algorithm; SCA, Sine Cosine Algorithm; SCSO, Sand Cat Swarm Optimization.

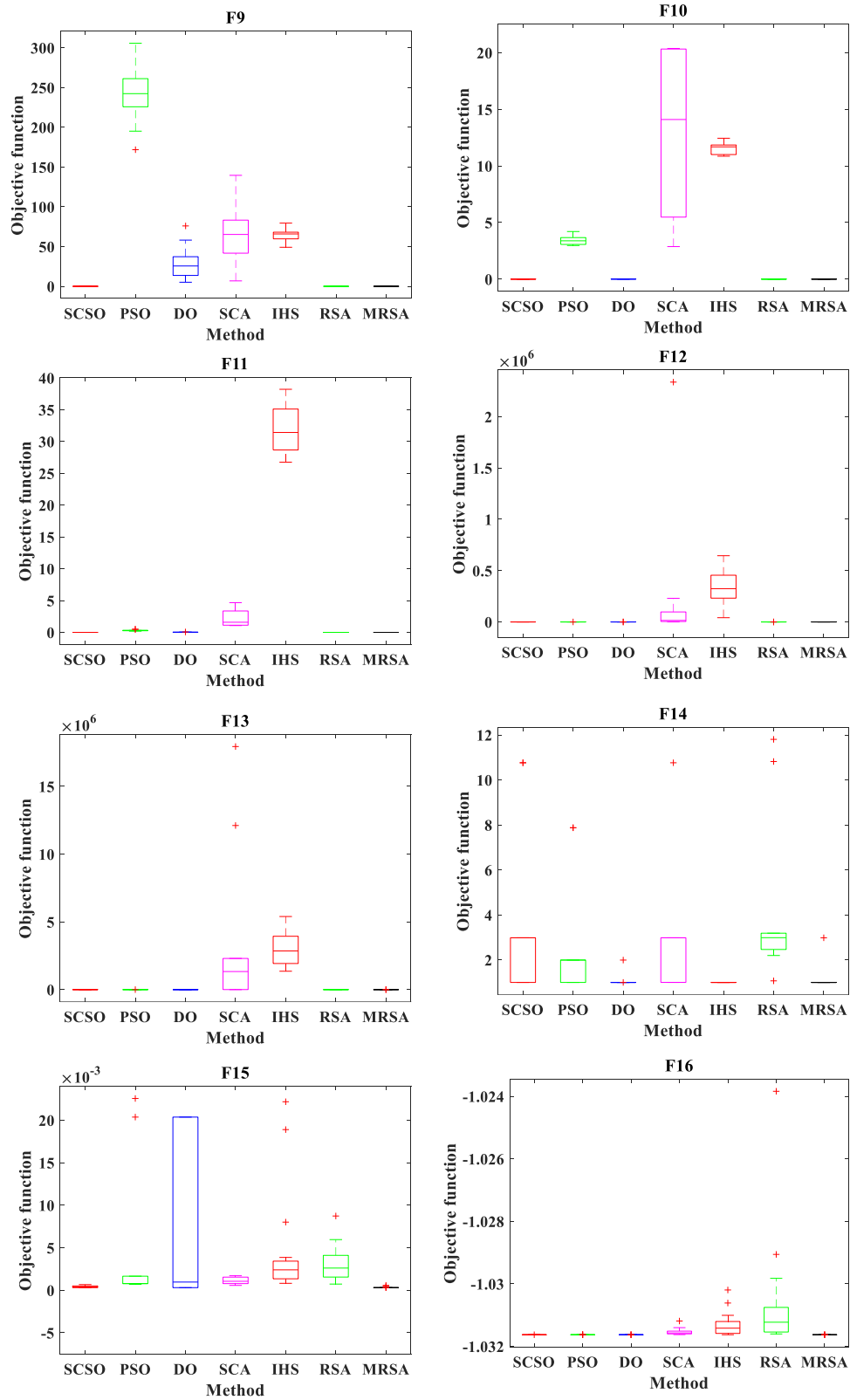


FIGURE 4 (Continued).

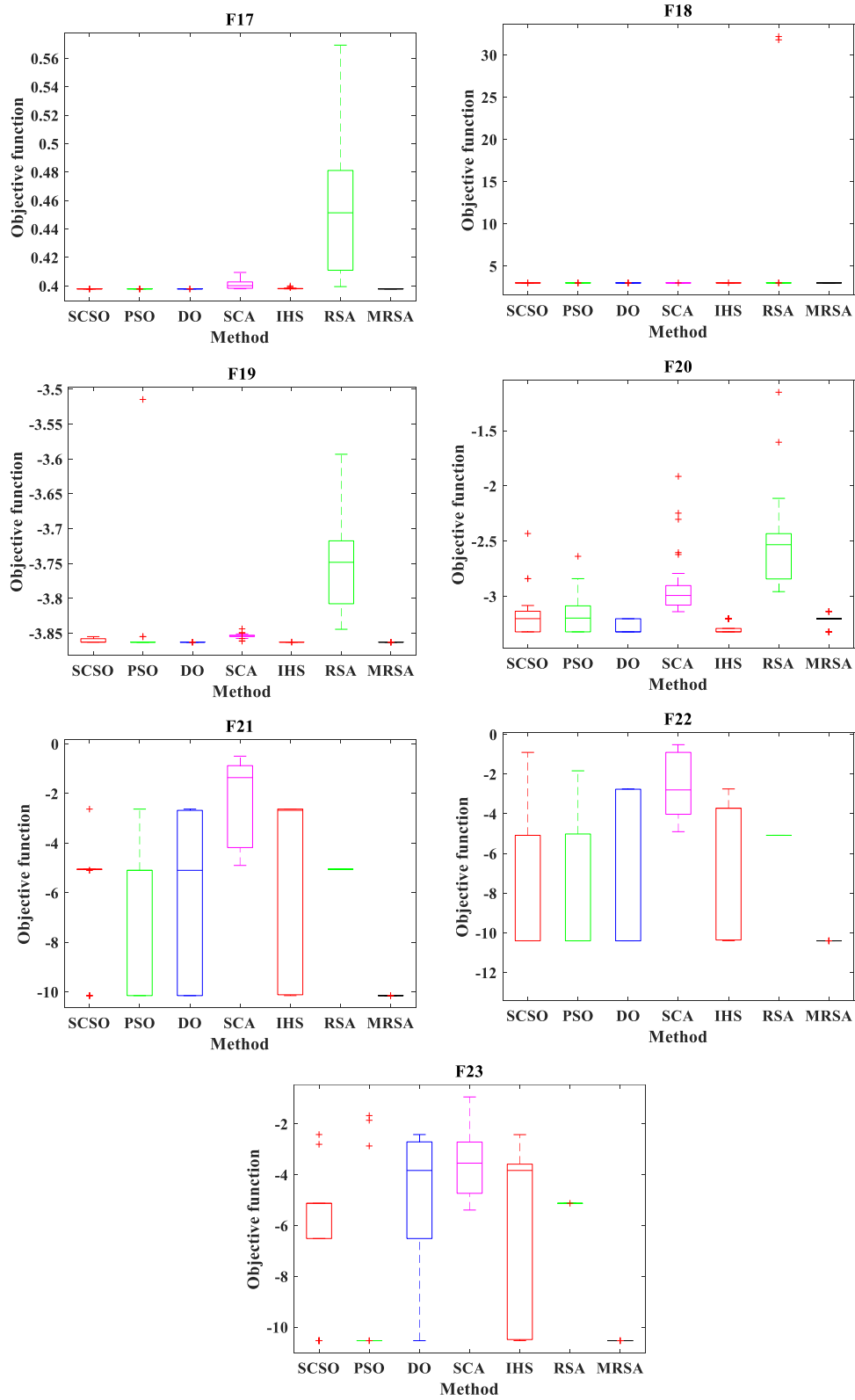


FIGURE 4 (Continued).

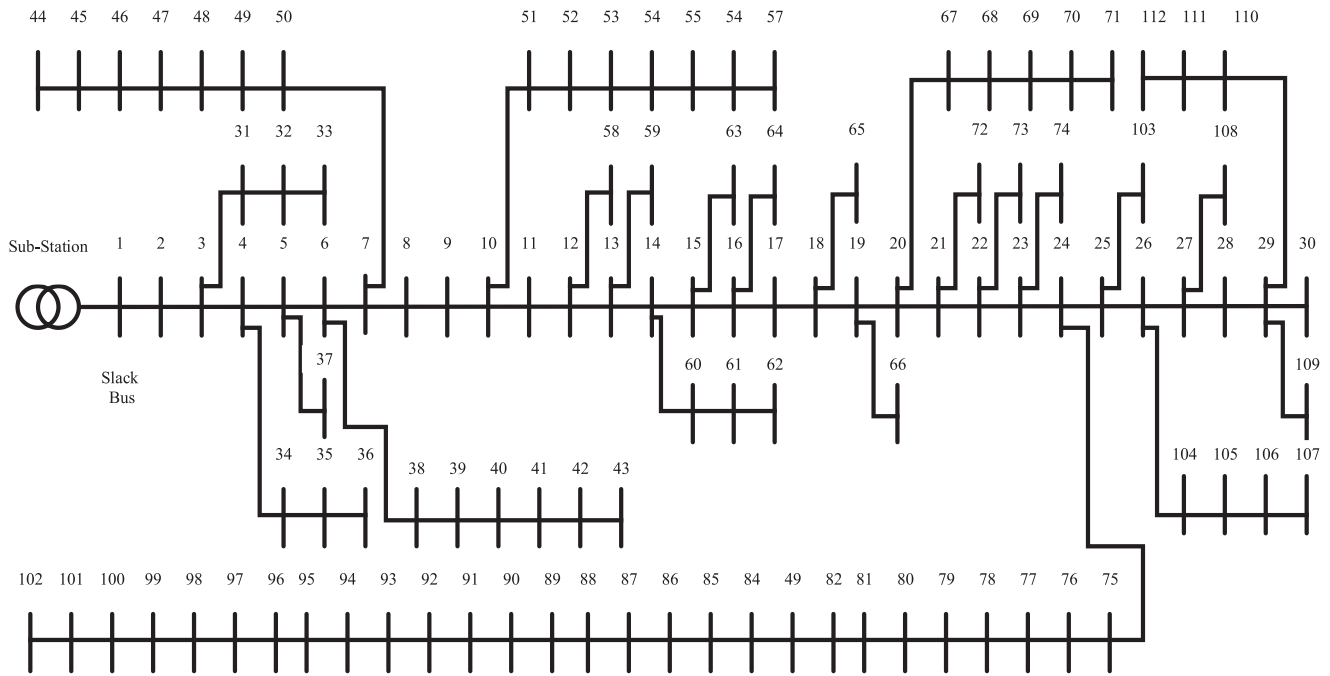


FIGURE 5 Schematic diagram of the 112-bus Algerian distribution network in the base case.

percentage of the j th element in the current solution compared with the j th element in the best-obtained solution is denoted by $P_{(i,j)}$, and is calculated using Equation (41). $R_{(i,j)}$ is a parameter utilized to shrink the search space, and its value is determined using Equation (39).

5 | MODIFIED REPTILE SEARCH ALGORITHM

The suggested MRSA is based on two improvement methods. The first modification aims to improve the exploration phase of the RSA using the fitness-distance balance (FDB) approach. The FDB is an efficient selection method that can guide the algorithm to the global solution.⁵⁰⁻⁵³ The FDB selection method is based on score values of the solution candidates. Then, the locations of the crocodiles are modified based on the fitness values and the distance between the candidates and the best solution. The distance values are calculated as follows:

$$DS_i = \frac{1}{\sqrt{(x_i^1 - Best^1)^2 + (x_i^2 - Best^2)^2 + \dots + (x_i^d - Best^d)^2}} \quad (44)$$

Then, construct the vectors of the fitness and the distance values as follows:

$$DS = [DS_1, DS_2, \dots, DS_n], \quad (45)$$

$$F = [F_1, F_2, \dots, F_n]. \quad (46)$$

Then the distance and the fitness value can be normalized as follows:

$$normDS_i = \frac{DS_i - \min(DS)}{\max(DS) - \min(DS)}m, \quad (47)$$

$$normF_i = \frac{F_i - \min(F)}{\max(F) - \min(F)}, \quad (48)$$

where \min and \max are the minimum and maximum in the distance and the fitness vectors. The following formula is used to calculate the FDB score:

$$FDB\ score_i = \alpha * (1 - normF_i) + (1 - \alpha) * normDS_i. \quad (49)$$

In which

$$\alpha = 0.5 * \left(1 + \frac{t}{T_{max}}\right). \quad (50)$$

The second modification is based on boosting the exploitation phase of the RSA technique by updating the locations of the crocodiles around the best solution using the Levy flight distribution according to (51).⁵⁴⁻⁵⁷

$$x_{(i,j)}(t + 1) = r_3 Best(t) - r_4 x_{(i,j)}(t) + C_1 \cdot L_F \cdot (x_{(r,j)}(t) - x_{(i,j)}(t)), \tag{51}$$

$$L_F = 0.05 \times \frac{u \times \sigma}{|v|^{1/\beta}}. \tag{52}$$

In which

$$\sigma = \left(\frac{\Gamma(1 + \beta) \times \sin(\pi\beta/2)}{\Gamma((1 + \beta)/2) \times \beta \times 2^{(\beta-1)/2}} \right)^{1/\beta}, \tag{53}$$

where r_3 and r_4 refer to a random value in the range $(0, 1)$. $x_{(i,j)}(t)$ and $x_{(r,j)}(t)$ represent the current location of the crocodiles and the best location, respectively. $C_1 = 2r_4(1 - T/T_{max})$ represents an operator that measures the intensity of the Levy flight. L_F is the Levy flight function which can be measured as follows:

where u and v denote random values that can be obtained from the normal distribution. β refers to a constant that is 1.5.

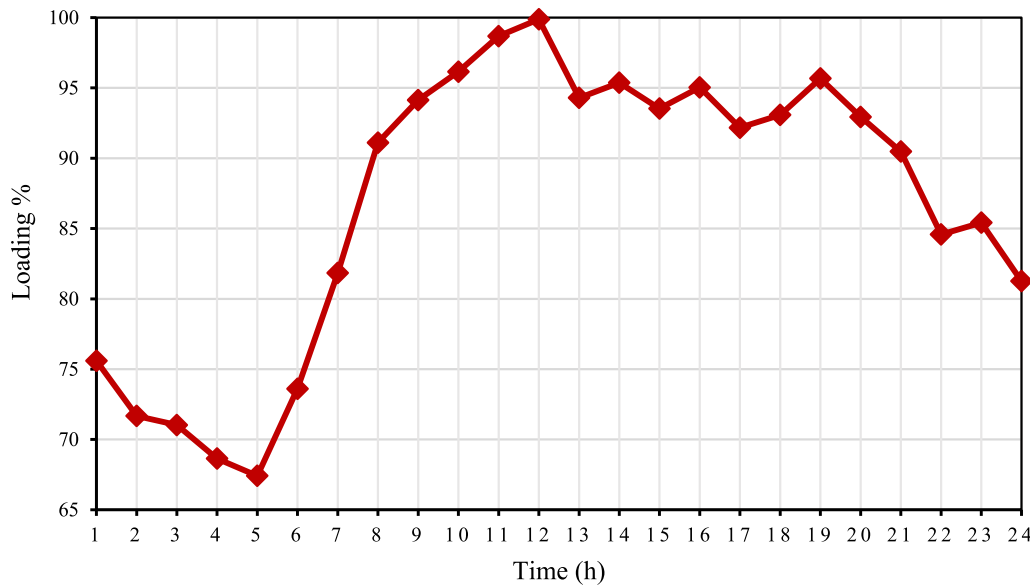


FIGURE 6 Expected load profile.

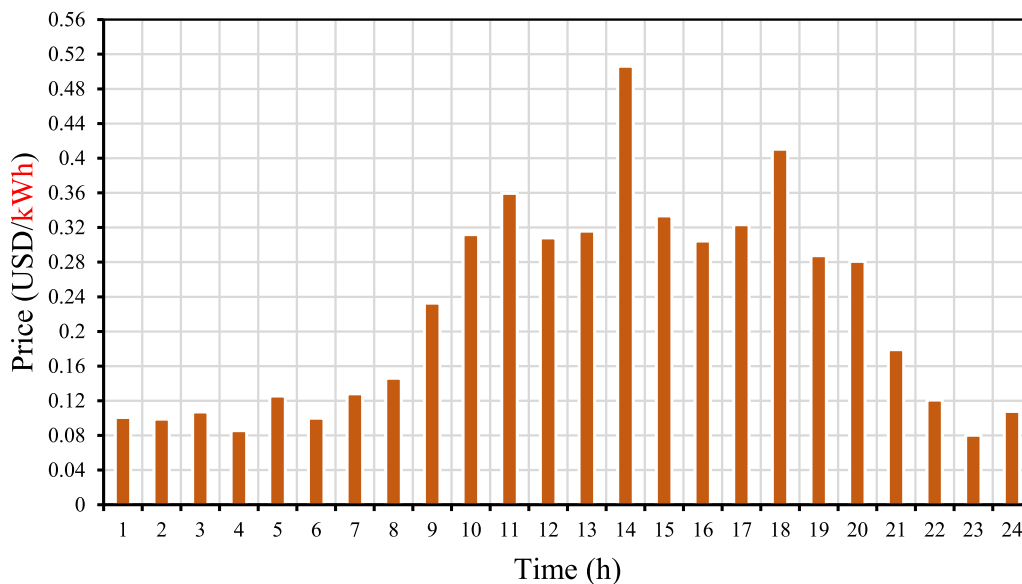


FIGURE 7 Expected price profile.

Figure 1 shows the MRSA for the optimal operation solution. The methodology for solving the stochastic optimal operation of a distribution grid is depicted in Figure 2.

6 | SIMULATION RESULTS

The suggested MRSA is applied to solving the real 112-bus Algerian DN. Initially, The proposed approach's performance was assessed through a comparison with other established optimization methods, such as SCSO,²⁹ PSO,³⁰ DO,³¹ SCA,³² IHS,³³ and the conventional RSA.²⁸ All the algorithms,

including the proposed MRSA, were programmed in MATLAB software (MATLAB R2019b) and executed on a computer with an Intel i7, 2.5 GHz CPU, and 6 GB RAM. The studied cases are presented as follows:

6.1 | Validation of the MRSA technique on standard benchmark functions

Here, the proposed MRSA is utilized for 23 classic functions, including the multimodal, unimodal, and fixed-dimension multimodal functions which have been

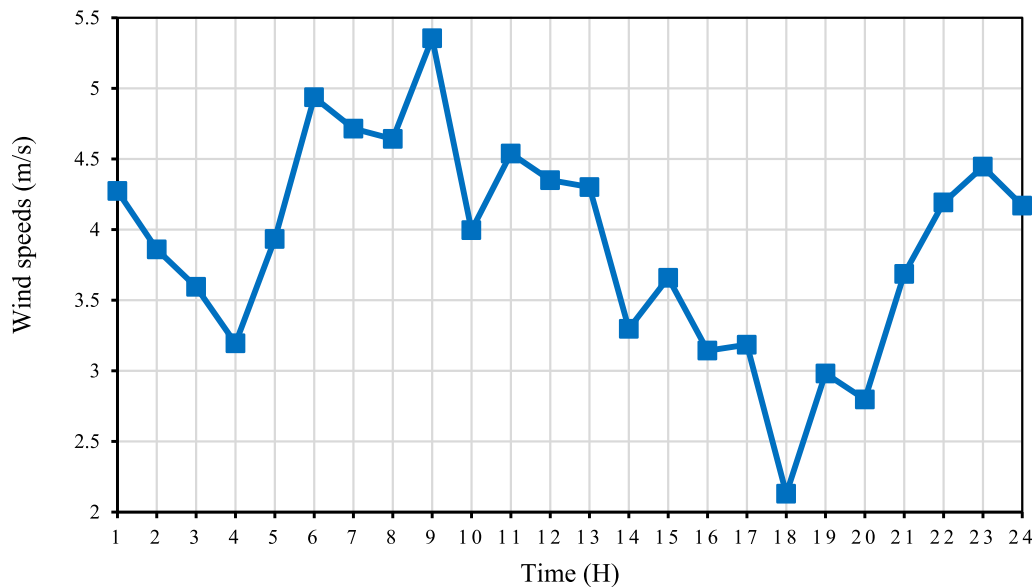


FIGURE 8 Expected wind speeds.

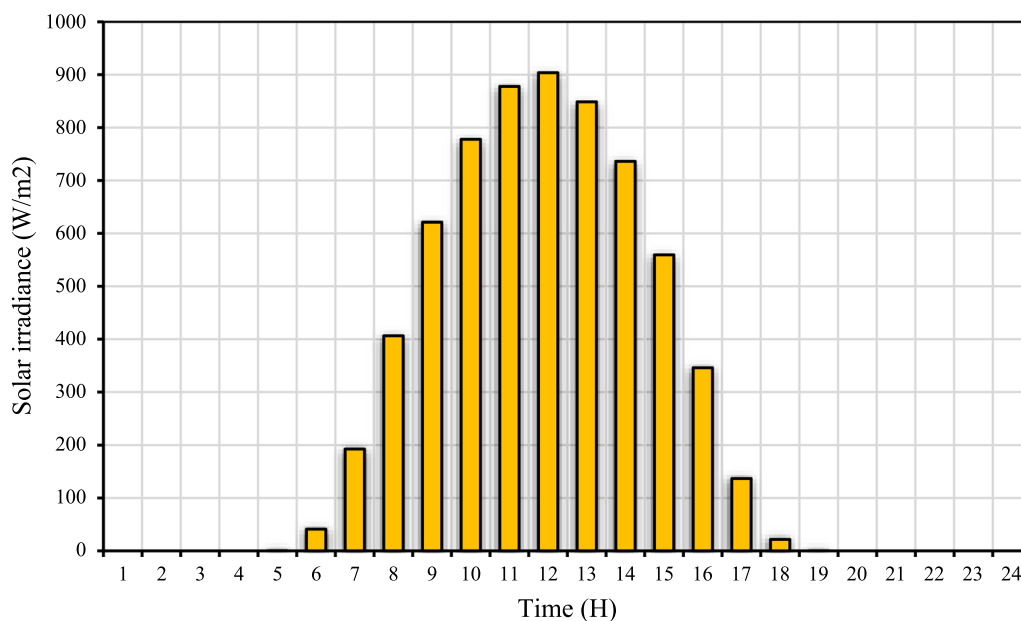


FIGURE 9 Expected solar irradiance.

listed in Appendix A.^{58,59} For all cases, the parameters are set according to Table 2 and the obtained results are represented over 30 run times.

6.2 | Statistical results analysis

This section depicts the performance of the proposed MRSA compared SCSO,²⁹ PSO,³⁰ DO,³¹ SCA,³² IHS,³³ and the conventional RSA.²⁸ Table 3 shows the statistical results, including the mean, the worst, the average, the best, and the Wilcoxon p value between the proposed MRSA and the other algorithms. According to Table 3,

the proposed MRSA optimizer is superior in terms of the mean, best, and worst values for the F1–F4, and F17–F23 while the obtained results for the reported algorithms are similar for F17–F23. In addition to that for F15 and F5, the RSA is better than MRSA in the value of the best score but the mean value of the MRSA is better. The p values of the Wilcoxon test compared with MRSA and the other optimizers are included in the 7th column of Table 3. When the p value is less than 5%, it is a significant difference between algorithms.⁶⁰ On the opposite of that when is more than 5%, no significant difference between optimizers. In addition to that if the results of different algorithms are identical, the p value

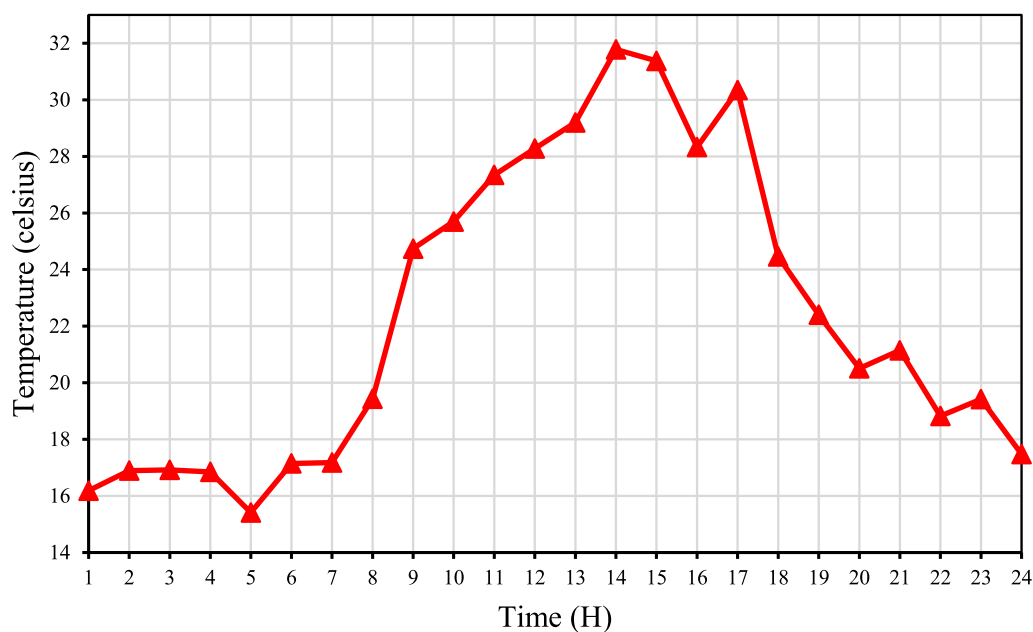


FIGURE 10 Expected temperature.

TABLE 4 Constraints and the cost coefficients.

Parameter	Value	Parameter	Value
The investment cost of PV (K_{PV}) ⁶³	770 USD/kW	The investment cost of WT (K_{WT}) ⁶⁴	1400 USD/kW
The maintenance and operation costs of PV ($K_{PV}^{O\&M}$) ⁶³	0.01 USD/kWh	The maintenance and operation costs of WT ($Co_{WT}^{O\&M}$) ⁶⁴	0.01 USD/kWh
The interest rate of PV (β_{PV}) ⁶³	10%	The interest rate of WT (β_{WT}) ⁶⁴	10%
The lifetime of PV (NP_{PV}) ⁶³	20	The lifetime of WT (NP_{WT}) ⁶⁴	20
The energy loss cost (K_{Loss}) ⁶⁵	0.06 USD/kWh		
<i>The system constraints</i>			
Voltage boundaries			0.95 p. u. $\leq V \leq$ 1.05 p. u.
PV and WT sizes			$0 \leq PV, WT \leq$ 3367.60 kW
PF of the WT			$0.7 \leq PF \leq$ 1

Abbreviations: PF, power flow; PV, photovoltaic; WT, wind turbine.

TABLE 5 Energy management results of Algerian distribution network.

Item	Without RERs	MRSA	RSA
Energy losses (kWh)	2.4901E + 03	1.9064E + 03	2.0017E + 03
Purchased power from grid (kW)	7.2657E + 04	4.4704E + 04	4.7329E + 04
Optimal location of PVs	–	81	46
		82	56
		102	103
Optimal location of WTs	–	5	35
		95	94
		112	105
Optimal area of the solar module (m ²)	–	4310	3152
		4000	2915
		5000	4592
Optimal size WTs (kW)	–	1000	750
		250	750
		250	250
Optimal PF of WTs	–	1	0.9178
		1	0.8430
		1	0.8243
Total annual energy loss cost (USD)	5.4533E + 04	4.1751E + 04	4.3838E + 04
Total annual purchased energy cost (USD)	6.2170E + 06	3.3349E + 06	3.6868E + 06
Total cost of PVs and WTs	–	1.5504E + 06	1.3425E + 06
$\sum VD$ (p.u.)	77.1022	60.4007	65.5820
$\sum VSI$ (p.u.)	2.3699E + 03	2.4314E + 03	2.4121E + 03
Total annual cost (USD)	6.2715E + 06	4.9270E + 06	5.0731E + 06

Note: Bold values indicate the best obtained solutions.

Abbreviations: MRSA, Modified Reptile Search Algorithm; PF, power flow; PV, photovoltaic; RESs, Renewable Energy Sources; RSA, Reptile Search Algorithm; WT, wind turbine.

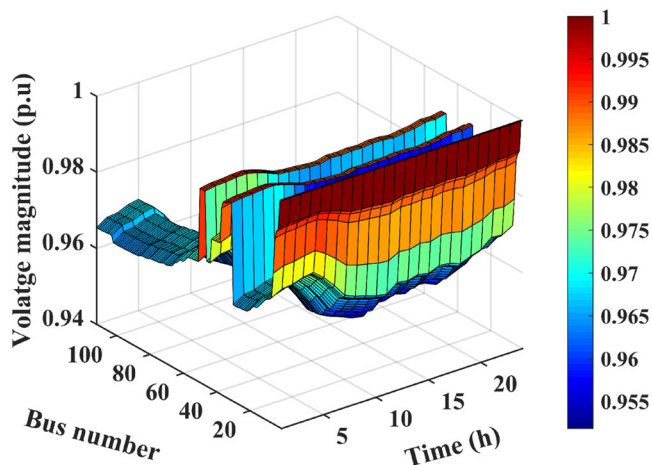


FIGURE 11 Voltage profile for the 112-bus Algerian distribution network without a hybrid system.

will be N/A. From the p value, it is clear that the proposed MRSA has significant difference compared with SCSO, PSO, DO, SCA, IHS, and the standard RSA for most of the studied benchmark functions, the population size and maximum iteration for all algorithms are 30 and 300, respectively.

6.3 | Convergence curves analysis

The convergence curves of the MRSA and other reported techniques including SCSO,²⁹ PSO,³⁰ DO,³¹ SCA,³² IHS,³³ and the conventional RSA²⁸ can be realized from Figure 3. According to the convergence curves, the proposed MRSA has the best convergence speed for the fixed-dimension functions, the unimodal functions, and

the multimodal functions. In addition to that, the suggested MRSA is superior and converged to the optimal solution faster than the conventional RSA due to the proposed modifications which can boost the exploration and exploitation phases of the proposed algorithm.

6.4 | Boxplot analysis

Boxplots are ideal for displaying data distributions in quartiles that can be used to show the characteristics of

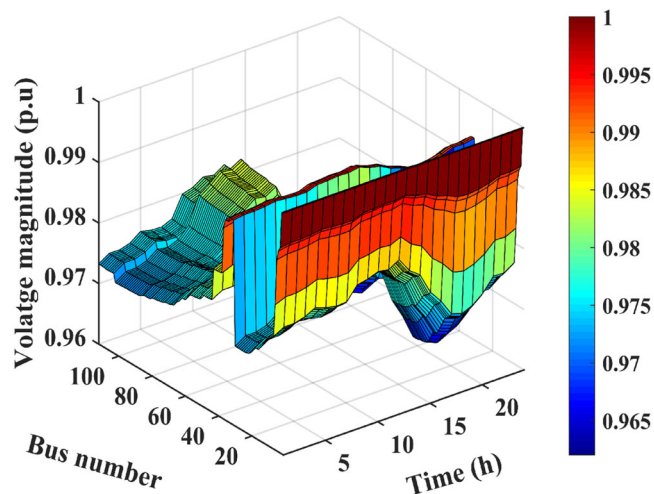


FIGURE 12 Voltage profile for the 112-bus Algerian distribution network with a hybrid system.

data distribution. Figure 4 depicts the Boxplots of the studied MRSA and the other reported optimization algorithms. It is obvious that the boxplots of the MRSA are narrower compared with the other optimizers.

6.5 | Solving the operation problem of Algerian DN using the proposed algorithm

In this section, the proposed MRSA is applied to solve the optimal operation and determine the best location for solar PV unit ratings and the WTs on 112-bus Algerian DN. The system, shown in Figure 5, consists of 112 buses and 111 branches with a cumulative load of 3367.60 kW and 3725.70 kVAR. The meteorological data for the wind speed, temperature, and solar radiation are collected over a period of 3 years from Ehsan and Yang.⁶¹ Also, the load demand data are collected for 3 years which given in Kaur et al.⁶² To validate the effectiveness of the proposed MRSA algorithm, the obtained results have been with those by other meta-heuristic optimization algorithms, including RSA, SCSO, DE, PSO, SCA, and IHS. To ensure a fair and valid comparison, the maximum number of iterations and populations selected for the proposed algorithms were set at 60 and 25, respectively. The presence of uncertainties, including load variations, wind speed, energy price, temperature, and solar irradiance, were considered in accordance with the methodology outlined in Section 3. Figure 6 illustrates the expected day-ahead load demand, while Figure 7 displays the market price for purchasing energy. In addition,

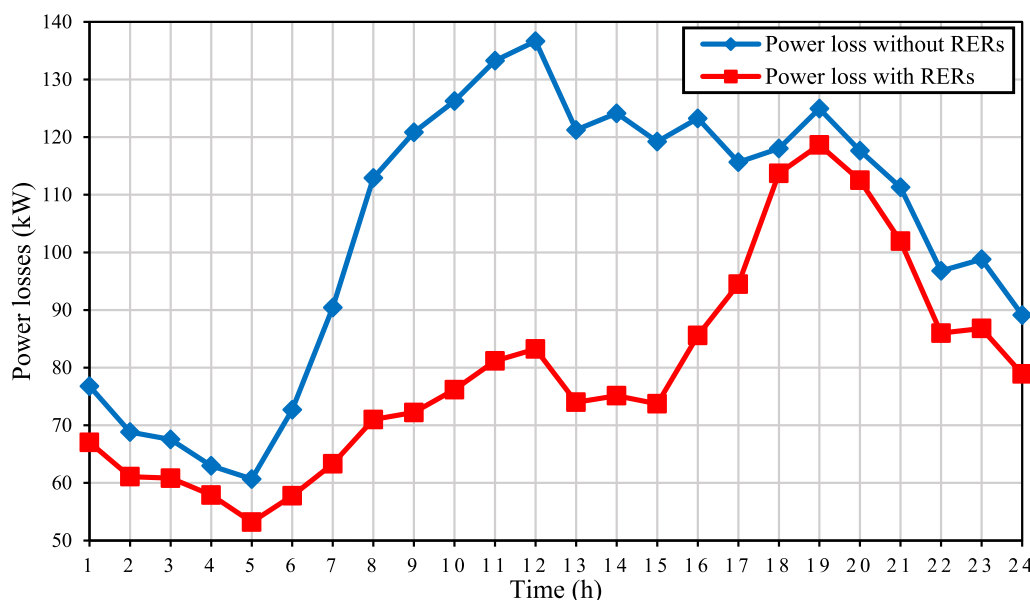


FIGURE 13 Power losses without and with RERs for the 112-bus Algerian DN. DN, distribution network; RESs, Renewable Energy Sources.

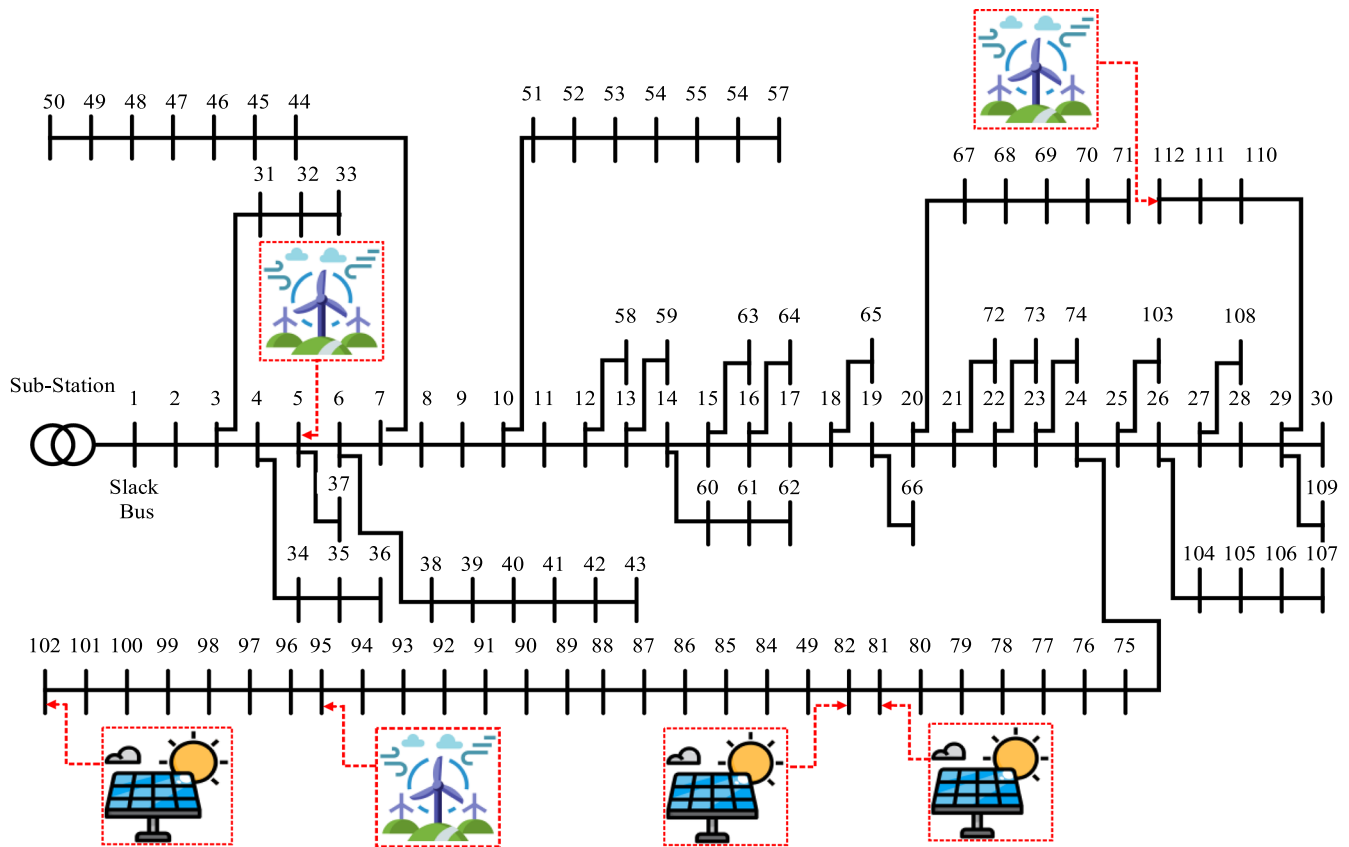


FIGURE 14 Schematic diagram of the 112-bus Algerian distribution network after integration renewable energy resources.

TABLE 6 Simulation results of objective function for applied algorithms.

Algorithm	Best	Worst	Average	SD
SCSO	0.591805	0.612766	0.600848	0.007993
PSO	0.598368	0.610271	0.604014	0.004717
DO	0.592609	0.616277	0.602314	0.009906
SCA	0.599937	0.616666	0.605769	0.006643
IHS	0.591025	0.60109	0.594352	0.003926
RSA	0.617207	0.645338	0.633937	0.010721
MRSA	0.58876	0.598005	0.592394	0.003944

Note: Bold values indicate the best obtained solutions.

Abbreviations: DO, Dandelion Optimizer; IHS, improved harmony search; MRSA, Modified Reptile Search Algorithm; PSO, particle swarm optimization; RSA, Reptile Search Algorithm; SCA, Sine Cosine Algorithm; SCSO, Sand Cat Swarm Optimization.

Figures 8–10 present the expected wind speed, irradiance, and temperature, respectively. Table 4 details the cost coefficients for RERs as well as the operational limitations.

The main objective of this paper is to optimize the total annual cost while improving system performance.

Initially, the base case was considered without any RERs integrated into the DN. The results showed that the total annual purchased energy from the grid was $7.2657E + 04$ kWh, with energy losses of $2.4901E + 03$ kW. The total purchase energy cost was $6.2170E + 06$ USD, and the energy loss cost was $5.4533E + 04$ USD, resulting in a total annual cost of $6.2715E + 06$ USD. The summation of the VD was 77.1022 p.u. and the VSI was $2.3699E + 03$ p.u. Table 5 shows the simulation results which have been obtained by different algorithms. According to Table 5, with the application of the proposed MRSA with the ideal allocation of the RERs, the total annual cost has been from $6.2715E + 06$ to $4.9270E + 06$ USD and the voltage deviations have been reduced from 77.1022 to 60.4007 p.u., while VSI has been improved from $2.3699E + 03$ to $2.4314E + 03$ p.u. The system voltage profiles with and without RERs are provided in Figures 11 and 12. Judging from Figures 11 and 12, the voltage profile was enhanced considerably with the inclusion of the PV units and the WTs. Additionally, as seen in Figure 13, the power losses have been significantly decreased. The optimal locations of PV units in the DN are identified as 81, 82, and 102, and the optimal locations of WTs are identified as 5, 95, and 112, respectively as shown in Figure 14. The WTs ratings are 1000, 250, and 250 kW, respectively, while the

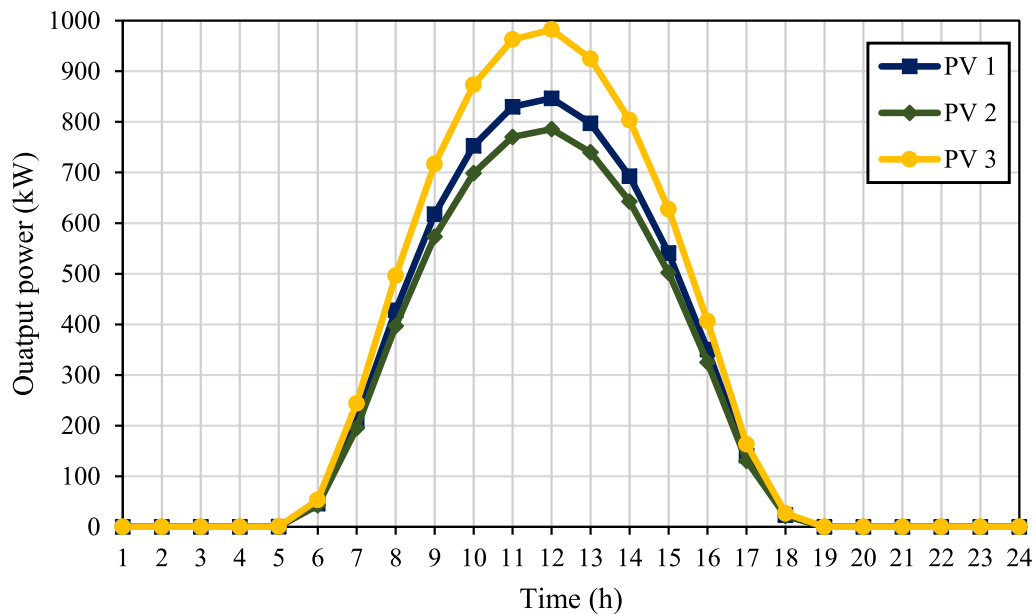


FIGURE 15 Hourly output power of PV units in the 112-bus Algerian DN. DN, distribution network; PV, photovoltaic;

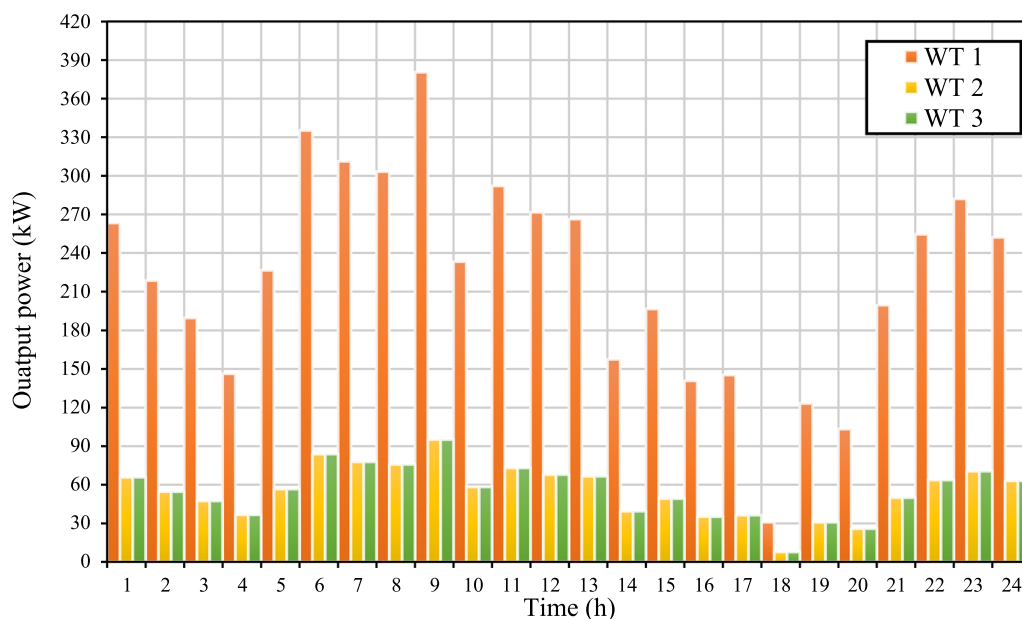


FIGURE 16 The hourly output power of WT units for the 112-bus Algerian DN. DN, distribution network; WT, wind turbine.

corresponding area of the solar modules are 4310, 4000, and 5000 m². The statistical outcomes for the objective function achieved through various optimization techniques are tabulated in Table 5. As depicted in Table 6, the results obtained by the proposed MRSA algorithm outperform other optimization techniques in terms of the mean, best, and worst values. The power output of the PV units is illustrated in Figure 15, indicating that their yields fluctuate continuously with irradiance variations. Similarly, the generated powers of the WT vary with changes in wind speed, as demonstrated in Figure 16.

7 | CONCLUSIONS

This paper solved the OOP of a real 112-bus Algerian DN with ideal integration of the RERs, including the PV units and the WTs using a new MRSA. The proposed MRSA is based on the FDB method and the Levy flight motion selection strategies. The optimal operation was solved by considering the uncertainties of the price, the load, the wind speed, temperature, and the solar irradiance. The proposed MRSA has been applied and tested on standard benchmark functions and the

obtained results were compared with other optimization algorithms, including the SCSSO, DE, PSO, SCA, IHS, and the standard RSA. The numerical results of optimal inclusion of the RERs using the proposed MSA show that the total cost has been reduced from $6.2715E + 06$ to $4.9270E + 06$ USD, the VD has been reduced from 77.1022 to 60.4007 p.u., and an enhancement in VSI has been enhanced from $2.3699E + 03$ to $2.4314E + 03$ p.u. in comparison to the base case. In addition, the findings demonstrate that the proposed MRSA algorithm for solving the optimal operation surpasses other optimization techniques, including SCSSO, DE, PSO, SCA, IHS, and the standard RSA, in terms of performance and effectiveness. However, this study has certain limitations, such as the absence of considerations for energy storage systems and electric vehicles (EVs). Future work will expand to encompass energy management in distribution systems, including various energy storage systems, like, batteries, compressed air, and Superconducting Magnetic Energy Storage, as well as incorporating EV charging stations.

ORCID

Ahmed T. Hachemi  <http://orcid.org/0000-0002-6808-9254>

Salah Kamel  <http://orcid.org/0000-0001-9505-5386>

Francisco Jurado  <http://orcid.org/0000-0001-8122-7415>

REFERENCES

- Rahman A, Farrok O, Mejbaul Haque Md. Environmental impact of renewable energy source based electrical power plants: solar, wind, hydroelectric, biomass, geothermal, tidal, ocean, and osmotic. *Renewable Sustainable Energy Rev.* 2022;161:112279.
- Zishan F, Mansouri S, Abdollahpour F, Grisales-Noreña LF, Montoya OD. Allocation of renewable energy resources in distribution systems while considering the uncertainty of wind and solar resources via the multi-objective salp swarm algorithm. *Energies.* 2023;16(1):474.
- Hachemi A, Sadaoui F, Arif S. Optimal location and sizing of capacitor banks in distribution systems using grey wolf optimization algorithm. In: *Advanced Computational Techniques for Renewable Energy Systems*. Springer; 2023:719-728.
- Dashtaki AA, Hakimi SM, Hasankhani A, Derakhshani G, Abdi B. Optimal management algorithm of microgrid connected to the distribution network considering renewable energy system uncertainties. *Int J Electr Power Energy Syst.* 2023;145:108633.
- Ahmed A, Nadeem MF, Kiani AT, Ullah N, Khan MA, Mosavi A. An improved hybrid approach for the simultaneous allocation of distributed generators and time varying loads in distribution systems. *Energy Rep.* 2023;9:1549-1560.
- Kellogg W, Nehrir M, Venkataramanan G, Gerez V. Optimal unit sizing for a hybrid wind/photovoltaic generating system. *Electr Power Syst Res.* 1996;39(1):35-38.
- Mansouri N, Lashab A, Guerrero JM, Cherif A. Photovoltaic power plants in electrical distribution networks: a review on their impact and solutions. *IET Renewable Power Gener.* 2020;14(12):2114-2125.
- Mansouri N, Lashab A, Sera D, Guerrero JM, Cherif A. Large photovoltaic power plants integration: a review of challenges and solutions. *Energies.* 2019;12(19):3798.
- Prakash P, Khatod DK. Optimal sizing and siting techniques for distributed generation in distribution systems: a review. *Renewable Sustainable Energy Rev.* 2016;57:111-130.
- Zellagui M, Lasmari A, Settoul S, El-Sehiemy RA, El-Bayeh CZ, Chenni R. Simultaneous allocation of photovoltaic DG and DSTATCOM for techno-economic and environmental benefits in electrical distribution systems at different loading conditions using novel hybrid optimization algorithms. *Int Trans Electr Energy Syst.* 2021;31(8):e12992.
- Venkatesan C, Kannadasan R, Alsharif MH, Kim M-K, Nebhen J. A novel multiobjective hybrid technique for siting and sizing of distributed generation and capacitor banks in radial distribution systems. *Sustainability.* 2021;13(6):3308.
- Hemeida MG, Alkhalaf S, Senjyu T, Ibrahim A, Ahmed M, Bahaa-Eldin AM. Optimal probabilistic location of DGs using Monte Carlo simulation based different bio-inspired algorithms. *Ain Shams Eng J.* 2021;12(3):2735-2762.
- Rathore A, Patidar NP. Optimal sizing and allocation of renewable based distribution generation with gravity energy storage considering stochastic nature using particle swarm optimization in radial distribution network. *J Energy Storage.* 2021;35:102282.
- El Sehiemy RA, Selim F, Bentouati B, Abido MA. A novel multi-objective hybrid particle swarm and salp optimization algorithm for technical-economical-environmental operation in power systems. *Energy.* 2020;193:116817.
- Ahmed D, Ebeed M, Ali A, Alghamdi AS, Kamel S. Multi-objective energy management of a micro-grid considering stochastic nature of load and renewable energy resources. *Electronics.* 2021;10(4):403.
- Thokar RA, Gupta N, Niazi KR, Swarnkar A, Sharma S, Meena NK. Optimal integration and management of solar generation and battery storage system in distribution systems under uncertain environment. *Int J Renewable Energy Res.* 2020;10(1):11-12.
- Biswal SR, Shankar G. Simultaneous optimal allocation and sizing of DGs and capacitors in radial distribution systems using SPEA2 considering load uncertainty. *IET Gener Transm Distrib.* 2020;14(3):494-505.
- Hadidian-Moghaddam MJ, Arabi-Nowdeh S, Bigdeli M, Azizian D. A multi-objective optimal sizing and siting of distributed generation using ant lion optimization technique. *Ain Shams Eng J.* 2018;9(4):2101-2109.
- Ahmed A, Nadeem MF, Sajjad IA, Bo R, Khan IA, Raza A. Probabilistic generation model for optimal allocation of wind DG in distribution systems with time varying load models. *Sustainable Energy Grids Networks.* 2020;22:100358.
- Rao BN, Abhyankar A, Senroy N. Optimal placement of distributed generator using Monte Carlo simulation. In: *2014 Eighteenth National Power Systems Conference (NPSC)*. IEEE; 2014:1-6.

21. Ullah K, Hafeez G, Khan I, Jan S, Javaid N. A multi-objective energy optimization in smart grid with high penetration of renewable energy sources. *Appl Energy*. 2021;299:117104.
22. Ali S, Ullah K, Hafeez G, Khan I, Albogamy FR, Haider SI. Solving day-ahead scheduling problem with multi-objective energy optimization for demand side management in smart grid. *Eng Sci Technol Int J*. 2022;36:101135.
23. Hafeez G, Wadud Z, Khan IU, et al. Efficient energy management of IoT-enabled smart homes under price-based demand response program in smart grid. *Sensors*. 2020;20(11):3155.
24. Hafeez G, Islam N, Ali A, Ahmad S, Usman M, Alimgeer KS. A modular framework for optimal load scheduling under price-based demand response scheme in smart grid. *Processes*. 2019;7(8):499.
25. Sakr WS, El-Sehiemy RA, Azmy AM. Adaptive differential evolution algorithm for efficient reactive power management. *Appl Soft Comput*. 2017;53:336-351.
26. Ginidi A, Ghoneim SM, Elsayed A, El-Sehiemy R, Shaheen A, El-Fergany A. Gorilla troops optimizer for electrically based single and double-diode models of solar photovoltaic systems. *Sustainability*. 2021;13(16):9459.
27. Dhawale PG, Kamboj VK, Bath SK. A Levy flight based strategy to improve the exploitation capability of arithmetic optimization algorithm for engineering global optimization problems. *Trans Emerging Telecommun Technol*. 2023;34(4):e4739.
28. Abualigah L, Abd Elaziz M, Sumari P, Geem ZW, Gandomi AH. Reptile search algorithm (RSA): a nature-inspired meta-heuristic optimizer. *Expert Syst Appl*. 2022;191:116158.
29. Seyyedabbasi A, Kiani F. Sand Cat swarm optimization: a nature-inspired algorithm to solve global optimization problems. *Eng Comput*. 2022;39:2627-2651.
30. Kennedy J, Eberhart R. Particle swarm optimization. In: *Proceedings of the International Conference on Neural Networks (ICNN'95)*. Vol 4. IEEE; 1995:1942-1948.
31. Zhao S, Zhang T, Ma S, Chen M. Dandelion optimizer: a nature-inspired metaheuristic algorithm for engineering applications. *Eng Appl Artif Intell*. 2022;114:105075.
32. Mirjalili S. SCA: a sine cosine algorithm for solving optimization problems. *Knowl-Based Syst*. 2016;96:120-133.
33. Mahdavi M, Fesanghary M, Damangir E. An improved harmony search algorithm for solving optimization problems. *Appl Math Comput*. 2007;188(2):1567-1579.
34. Ebeed M, Ahmed D, Kamel S, et al. Optimal energy planning of multi-microgrids at stochastic nature of load demand and renewable energy resources using a modified Capuchin Search Algorithm. *Neural Comput Appl*. 2023;35:17645-17670.
35. Ramadan A, Ebeed M, Kamel S, Ahmed EM, Tostado-Véliz M. Optimal allocation of renewable DGs using artificial hummingbird algorithm under uncertainty conditions. *Ain Shams Eng J*. 2023;14(2):101872.
36. Asaad A, Ali A, Mahmoud K, et al. Multi-objective optimal planning of EV charging stations and renewable energy resources for smart microgrids. *Energy Sci Eng*. 2023;11(3):1202-1218.
37. Diaf S, Diaf D, Belhamel M, Haddadi M, Louche A. A methodology for optimal sizing of autonomous hybrid PV/wind system. *Energy Policy*. 2007;35(11):5708-5718.
38. Eltamaly AM, Mohamed MA, Alolah AI. A novel smart grid theory for optimal sizing of hybrid renewable energy systems. *Sol Energy*. 2016;124:26-38.
39. Purlu M, Turkay BE. Optimal allocation of renewable distributed generations using heuristic methods to minimize annual energy losses and voltage deviation index. *IEEE Access*. 2022;10:21455-21474.
40. Amin A, Ebeed M, Nasrat L, et al. Techno-economic evaluation of optimal integration of PV based DG with DSTATCOM functionality with solar irradiance and loading variations. *Mathematics*. 2022;10(14):2543.
41. Barnwal AK, Yadav LK, Verma MK. A multi-objective approach for voltage stability enhancement and loss reduction under PQV and P buses through reconfiguration and distributed generation allocation. *IEEE Access*. 2022;10:16609-16623.
42. Ali ES, Abd Elazim SM, Abdelaziz AY. Ant lion optimization algorithm for renewable distributed generations. *Energy*. 2016;116:445-458.
43. Akbari MA, Aghaei J, Barani M, et al. New metrics for evaluating technical benefits and risks of DGs increasing penetration. *IEEE Trans Smart Grid*. 2017;8(6):2890-2902.
44. Ali A, Raisz D, Mahmoud K, Lehtonen M. Optimal placement and sizing of uncertain PVs considering stochastic nature of PEVs. *IEEE Trans Sustainable Energy*. 2019;11(3):1647-1656.
45. Ebeed M, Ali A, Mosaad MI, Kamel S. An improved lightning attachment procedure optimizer for optimal reactive power dispatch with uncertainty in renewable energy resources. *IEEE Access*. 2020;8:168721-168731.
46. Zubo RH, Mokryani G, Abd-Alhameed R. Optimal operation of distribution networks with high penetration of wind and solar power within a joint active and reactive distribution market environment. *Appl Energy*. 2018;220:713-722.
47. Ozay C, Celiktas MS. Statistical analysis of wind speed using two-parameter Weibull distribution in Alaçatı region. *Energy Convers Manage*. 2016;121:49-54.
48. Jamal R, Zhang J, Men B, Khan NH, Ebeed M, Kamel S. Solution to the deterministic and stochastic optimal reactive power dispatch by integration of solar, wind-hydro powers using modified artificial hummingbird algorithm. *Energy Rep*. 2023;9:4157-4173.
49. Morstyn T, Teytelboym A, Hepburn C, McCulloch MD. Integrating P2P energy trading with probabilistic distribution locational marginal pricing. *IEEE Trans Smart Grid*. 2019;11(4):3095-3106.
50. Kahraman HT, Aras S, Gedikli E. Fitness-distance balance (FDB): a new selection method for meta-heuristic search algorithms. *Knowl-Based Syst*. 2020;190:105169.
51. Aras S, Gedikli E, Kahraman HT. A novel stochastic fractal search algorithm with fitness-distance balance for global numerical optimization. *Swarm Evol Comput*. 2021;61:100821.
52. Duman S, Kahraman HT, Guvenc U, Aras S. Development of a Lévy flight and FDB-based coyote optimization algorithm for global optimization and real-world ACOFP problems. *Soft Comput*. 2021;25:6577-6617.
53. Xu Y, Peng Y, Su X, Yang Z, Ding C, Yang X. Improving teaching-learning-based-optimization algorithm by a distance-fitness learning strategy. *Knowl-Based Syst*. 2022;257:108271.

54. Zhong C, Li G, Meng Z. Beluga whale optimization: a novel nature-inspired metaheuristic algorithm. *Knowl-Based Syst.* 2022;251:109215.
55. Mostafa A, Ebeed M, Kamel S, Abdel-Moamen MA. Optimal power flow solution using levy spiral flight equilibrium optimizer with incorporating CUPFC. *IEEE Access.* 2021;9:69985-69998.
56. Alhejji A, Ebeed Hussein M, Kamel S, Alyami S. Optimal power flow solution with an embedded center-node unified power flow controller using an adaptive grasshopper optimization algorithm. *IEEE Access.* 2020;8:119020-119037.
57. Ebeed M, Alhejji A, Kamel S, Jurado F. Solving the optimal reactive power dispatch using marine predators algorithm considering the uncertainties in load and wind-solar generation systems. *Energies.* 2020;13(17):4316.
58. Jamil M, Yang X-S. A literature survey of benchmark functions for global optimization problems. *arXiv preprint arXiv:1308.4008*, 2013.
59. Molga M, Smutnicki, C. Test functions for optimization needs. 2005;101:48.
60. Derrac J, García S, Molina D, Herrera F. A practical tutorial on the use of nonparametric statistical tests as a methodology for comparing evolutionary and swarm intelligence algorithms. *Swarm Evol Comput.* 2011;1(1):3-18.
61. Ehsan A, Yang Q. Optimal integration and planning of renewable distributed generation in the power distribution networks: a review of analytical techniques. *Appl Energy.* 2018;210:44-59.
62. Kaur S, Kumbhar G, Sharma J. A MINLP technique for optimal placement of multiple DG units in distribution systems. *Int J Electr Power Energy Syst.* 2014;63:609-617.
63. Gampa SR, Das D. Optimum placement and sizing of DGs considering average hourly variations of load. *Int J Electr Power Energy Syst.* 2015;66:25-40.
64. Augustine N, Suresh S, Moghe P, Sheikh K. Economic dispatch for a microgrid considering renewable energy cost functions. In: *2012 IEEE PES Innovative Smart Grid Technologies (ISGT)*. IEEE; 2012:1-7.
65. Sultana S, Roy PK. Optimal capacitor placement in radial distribution systems using teaching learning based optimization. *Int J Electr Power Energy Syst.* 2014;54:387-398.

How to cite this article: Hachemi A, Sadaoui F, Arif S, et al. Modified reptile search algorithm for optimal integration of renewable energy sources in distribution networks. *Energy Sci Eng.* 2023;11:4635-4665. doi:10.1002/ese3.1605

APPENDIX A: STUDIED OBJECTIVE TEST FUNCTIONS

See Tables A1–A3.

TABLE A1 Unimodal functions.

Function	Range	F_{min}
$f_1(k) = \sum_{j=1}^n k_j^2$	[-100, 100]	0
$f_2(k) = \sum_{j=1}^n k_j + \prod_{j=1}^n k_j $	[-10, 10]	0
$f_3(k) = \sum_{j=1}^n \left(\sum_{i=1}^j k_i \right)^2$	[-100, 100]	0
$f_4(k) = \max_j k_j , 1 \leq j \leq n$	[-100, 100]	0
$f_5(k) = \sum_{j=1}^{n-1} \left[100(k_{j+1} - k_j^2)^2 + (k_j - 1)^2 \right]$	[-30, 30]	0
$f_6(k) = \sum_{j=1}^{n-1} ([k_j + 0.5])^2$	[-100, 100]	0
$f_7(k) = \sum_{j=1}^n j k_j^4 + \text{random}(0, 1)$	[-1.28, 1.28]	0

TABLE A2 Multimodal functions.

Function	Range	F_{min}
$f_8(k) = \sum_{j=1}^n -k_j \sin(\sqrt{ k_j })$	$[-500, 500]$	$-418.9829 * 5$
$f_9(k) = \sum_{j=1}^n [k_j^2 - 10 \cos(2\pi k_j + 10)]$	$[-5.12, 5.12]$	0
$f_{10}(k) = -20 \exp\left(-0.2 \sqrt{\frac{1}{n} \sum_{j=1}^n k_j^2}\right) - \exp\left(\frac{1}{n} \sum_{j=1}^n \cos(2\pi k_j) + 20 + e\right)$	$[-32, 32]$	0
$f_{11}(k) = \frac{1}{4000} \sum_{j=1}^n k_j^2 - \prod_{j=1}^n \cos\left(\frac{k_j}{\sqrt{j}}\right) + 1$	$[-600, 600]$	0
$f_{12}(k) = \frac{\pi}{n} \left\{ 10 \sin(\pi z_1) + \sum_{j=1}^{n-1} (z_j - 1)^2 [1 + 10 \sin^2(\pi z_{j+1})] + (z_n - 1)^2 \right\} + \sum_{j=1}^n u(k_j, 10, 100, 4) z_j = 1 + \frac{k_j + 1}{4}$	$[-50, 50]$	0
$u(k_j, v, s, h) = \begin{cases} x(k_j - v)^h, & k_j > v, \\ 0, & -v < k_j < v, \\ x(-k_j - v)^h, & k_j < -v \end{cases}$		
$f_{13}(k) = 0.1 \left\{ \sin^2(3\pi k_1) + \sum_{j=1}^n (k_j - 1)^2 [1 + \sin^2(3\pi k_j + 1)] + (k_n - 1)^2 [1 + \sin^2(2\pi k_j)] \right\} + \sum_{j=1}^n u(k_j, 5, 100, 4)$	$[-50, 50]$	
$f_{14}(k) = -\sum_{j=1}^n \sin(k_j) \cdot \left(\sin\left(\frac{j \cdot k_j^2}{\pi}\right) \right)^{2h}, \quad h = 10$	$(0, \pi)$	-4.687
$f_{15}(k) = \left[e^{-\sum_{j=1}^n \left(\frac{k_j}{\beta}\right)^{2h}} - 2e^{-\sum_{j=1}^n k_j^2} \right] - \prod_{j=1}^n \cos^2 k_j, \quad h = 5$	$[-20, 20]$	-1
$f_{16}(k) = \left\{ \left[\sum_{j=1}^n \sin^2(k_j) \right] - \exp\left(-\sum_{j=1}^n k_j^2\right) \right\} \cdot \exp\left[-\sum_{j=1}^n \sin^2 \sqrt{ k_j }\right]$	$[-10, 10]$	-1

TABLE A3 Fixed-dimension multimodal benchmark functions.

Function	Dim	Range	F_{min}
$f_{14}(k) = \frac{1}{500} + \sum_{i=1}^{25} \frac{1}{i + \sum_{j=1}^2 (k_j - a_{ij})^6}$	2	$[-65, 65]$	1
$f_{15}(k) = \sum_{j=1}^{11} \left[b_j - \frac{k_j(b_j^2 + b_j k_2)}{b_j^2 + b_j k_3 + k_4} \right]^2$	4	$[-5, 5]$	0.00030
$f_{16}(k) = 4k_1^2 - 2.1k_1^4 + \frac{1}{3}k_1^6 + k_1 k_2 - 4k_2^2 + 4k_2^4$	2	$[-5, 5]$	-1.0316
$f_{17}(k) = \left(k_2 - \frac{5.1}{4\pi^2} k_1^2 + \frac{5}{\pi} k_1 - 6 \right)^2 + 10 \left(1 - \frac{1}{8\pi} \right) \cos k_1 + 10$	2	$[-5, 5]$	0.398
$f_{18}(k) = \left[1 + (k_1 + k_2 + 1)^2 (19 - 14k_1 + 3k_1^2 - 14k_2 + 6k_1 k_2 + 3k_2^2) \right] * \left[30 + (2k_1 - 3k_2)^2 (18 - 32k_1 + 12k_1^2 - 48k_2 + 36k_1 k_2 + 27k_2^2) \right]$	2	$[-2, 2]$	3
$f_{19}(k) = -\sum_{j=1}^4 c_j \exp\left(-\sum_{i=1}^3 a_{ji} (k_i - p_{ji})^2\right)$	3	$[1, 3]$	-3.86
$f_{20}(k) = -\sum_{j=1}^4 c_j \exp\left(-\sum_{i=1}^6 a_{ji} (k_i - p_{ji})^2\right)$	6	$[0, 1]$	-3.32
$f_{21}(k) = -\sum_{j=1}^5 [(k - a_j)(k - a_j)^T + c_j]^{-1}$	4	$[0, 10]$	-10.1532
$f_{22}(k) = -\sum_{j=1}^7 [(k - a_j)(k - a_j)^T + c_j]^{-1}$	4	$[0, 10]$	-10.4028
$f_{23}(k) = -\sum_{j=1}^{10} [(k - a_j)(k - a_j)^T + c_j]^{-1}$	4	$[0, 10]$	-10.5363